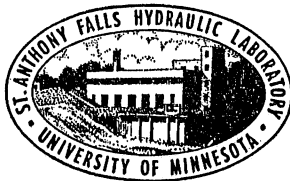


UNIVERSITY OF MINNESOTA
ST. ANTHONY FALLS HYDRAULIC LABORATORY

Project Report No. 119

The Influence of Drag Reducing Polymer Additives
on Surface Pressure Fluctuations on Rough Surfaces

by
JOHN M. KILLEN
and
JOHN A. ALMO



This research was sponsored by the Naval Ship Systems Command General Hydromechanics Research Program administered by the Naval Ship Research and Development Center under Contract N00014-67-A-0113-0007.

SEPTEMBER 1971
MINNEAPOLIS, MINNESOTA

Approved for public release; distribution unlimited

CONTENTS

	<u>Page</u>
List of Illustrations	v
List of Symbols	vii
Preface	ix
Abstract	xi
I. INTRODUCTION	1
II. EXPERIMENTAL PROCEDURE	3
III. BOUNDARY LAYER CHARACTERISTICS	5
IV. BOUNDARY LAYER MEASUREMENTS	7
V. BROAD BAND PRESSURE FLUCTUATIONS	8
VI. PRESSURE SPECTRA	8
VII. SUMMARY	13
List of References	15
Table I	17
Figures 1 through 22	21

LIST OF ILLUSTRATIONS

Figure		Page
1	Sketch of Test Tank with Rotating Cylinder in Place	23
2	Vortices between Rotating Cylinders	24
3	Mean Velocity Distribution for Type A and Type B Flow	25
4	Typical Velocity Profile	26
5	Shape Factor vs. Reynolds Number	27
6	Velocity Profile near Rotating Cylinder	28
7	Measured Cylinder Drag Coefficient	29
8	Comparison of Surface Pressure Fluctuation on a Rotating Cylinder and Buoyant Body	30
9	Integrated Root Mean Square Surface Pressure Fluctuation on a Smooth Surface	31
10	Integrated Root Mean Square Surface Pressure Fluctuation on a Rough Surface (0.018 in. diam. bead roughness, 1/8 in. diam. hydrophone, smooth surface)	32
11	Surface Pressure Fluctuation Spectra in Water on a Smooth Surface ...	33
12	Surface Pressure Fluctuation Spectra on a Smooth Surface with 50 ppmw Polyox 301 added to the water	34
13	Surface Pressure Fluctuation Spectra on a Smooth Surface with various concentrations of Polyox 301	35
14	Surface Pressure Fluctuation Spectra on a Smooth Surface with Large Change in Polyox 301 Concentration	36
15	Surface Pressure Fluctuation Spectra on Rough Surfaces - Water	37
16	Surface Pressure Fluctuation Spectra - Comparison of Roughness and Additive with Smooth Surface Condition	38
17	Surface Pressure Fluctuation Spectra on a Rough Surface with various concentrations of Polyox 301	39
18	Surface Pressure Fluctuation Spectra - Interaction between Roughness and Hydrophone in the presence of Polymer - Roughness $K = 0.018$, 100 ppmw Polyox 301	40
19	Surface Pressure Fluctuation Spectra - Interaction between Roughness and Hydrophone in Water Only, Roughness $K = 0.018$	41

[Continued]

Figure		Page
20	Surface Pressure Fluctuation Spectra on a Smooth Surface - Water Only ..	42
21	Surface Pressure Fluctuation Spectra as Influenced by Roughness and Drag Reducing Additive	43
22	Comparison of "Fitted" Curves to Four Experimental Conditions	44

LIST OF SYMBOLS

$$C_d = \text{Skin friction coefficient} = \frac{\tau_o}{\frac{\rho V^2}{2}}$$

H = Boundary layer shape factor = δ^*/θ or correlation parameter

K = Particle diameter, inches

K_g = Equivalent particle diameter

P' = Root mean square value of pressure fluctuation

R = Radius of cylinder, feet

$$R_\theta = \frac{V\theta}{\nu}$$

Reynolds Number = VR/ν

U = Average velocity at a distance r from the cylinder axis

$$U_\infty = V$$

$$U^* = \sqrt{\tau_o/\rho}$$

$$U^+ = U/\sqrt{\tau_o/\rho}$$

V = Cylinder surface velocity, fps

Y = Distance from cylinder surface

$$Y^+ = YU^*/\nu$$

ΔB = Displacement of U^+ profile

δ_{99} = Boundary layer thickness at $U = 0.01 V$

$$\delta^* = \text{Boundary layer displacement thickness} = \int_0^\delta \frac{U}{V} dy$$

$$\theta = \text{Boundary layer momentum thickness} = \int_0^\delta \left(1 - \frac{U}{V}\right) \frac{U}{V} dy$$

ρ = Fluid density in slugs

ν = Kinematic viscosity

τ_o = Average surface shear

$$\phi(\omega) = \frac{\phi(f)}{2\pi} = \frac{\overline{p'^2}}{2\pi(\text{Bandwidth})} \quad \text{where } \overline{p'^2} \text{ is the mean square pressure}$$

within one measured bandwidth

ω = Angular frequency or velocity

PREFACE

The work reported herein is an experimental effort to determine the effects of polymer additive and roughness on surface pressure fluctuations. The studies were sponsored by the Naval Ship Research and Development Center, Department of the Navy, under Contract N00014-67-A-0113-0007 and were carried out in the period between October 1967 and April 1970. Thanks are expressed to J. M. Wetzel and Edward Silberman for their review of the report and to Mrs. Shirley Kii for preparing the manuscript.

Raw data have not been presented in the report, but are available from the St. Anthony Falls Hydraulic Laboratory.

ABSTRACT

Experimental measurements were made to determine the effect of drag reducing polymer additives on the surface pressure fluctuations on smooth and rough surfaces in relative motion with water.

Changes in surface pressure fluctuation intensity were found to be closely related to changes in surface shear when shear change was caused by the addition of drag reducing polymer, by a change in surface roughness, or by both of these.

THE INFLUENCE OF DRAG REDUCING POLYMER ADDITIVES ON SURFACE PRESSURE FLUCTUATIONS ON ROUGH SURFACES

I. INTRODUCTION

Surface pressure fluctuations on surfaces in relative motion with a fluid have been the subject of considerable investigation with regard to vibration and noise of aircraft. Much interest has also arisen in surface pressure fluctuations as part of the more general phenomenon of turbulent flows, particularly as influenced by polymers. An extensive bibliography of current literature has been given by Skudrzyk and Haddle [1]*.

The majority of the experimental work on surface pressure fluctuations has been carried out in air. The few investigations in water [2, 3, 4, and 5] have shown no apparent difference in results from those in air when scaling has been appropriate.

The physical picture commonly used as an analog for the source of surface pressure fluctuations is that of an ensemble of vortices with their associated pressure distributions which are convected past a measuring point on the surface. The pressure pattern of the vortices as they are swept past the measuring point gives rise to a temporal variation of pressure at that point. Part of the measured pressure is due to the motion of the vortices and part to the temporal decay of the vortex and its pressure pattern. Pressure fluctuations due to turbulence production may also be present [6]. The eddies are assumed to arise from a "breakdown" process in the viscous sublayer. However, pressure measurements give evidence of components both from the sublayer and from the outer flow which have been convected near the measuring point [7].

The magnitude of the response of a surface hydrophone placed at the measuring point will depend on the pressure signature of the vortex modified by the relative sizes of the vortex and the hydrophone both along and across the flow [8] and by the relative distance of the vortex from the surface [9]. Measurements of the convection velocity of the pressure pattern past the hydrophone indicate that the vortices are moving roughly with the local stream velocity at their respective distances from the surface.

*Numbers in brackets refer to list of references on pages 15 and 16.

A relationship between the convection velocity and the size of the vortex becomes apparent, since it is possible for a smaller eddy, on the average, to occupy a position closer to the wall than a larger eddy, and it will as a result have a lower convection velocity. This is reflected in the fact that high-frequency pressure fluctuations associated with smaller eddies have lower convection velocities [7].

Drag reducing polymers have been shown to reduce drag through their effect in or near the viscous sublayer region. Meyers [10] has shown that one of the more easily observed effects is a thickening of the sublayer region. This can be determined from velocity profile measurements. The surface pressure fluctuations have a component arising in or transported through this region; consequently, it is reasonable to expect polymers to have an effect on surface pressure fluctuations also. A semi-theoretical study by White [11] predicts that wall pressure fluctuation will be reduced if shear is reduced by a polymer additive. White postulated in addition, however, that pressure fluctuations are also dependent on a parameter having a dimension of length which he called H . It is equal to the zero intercept distance from the origin of the correlation function $\overline{\left(\frac{\partial v}{\partial x} \frac{\partial v'}{\partial x'}\right)}$ in which v and v' are the velocity components normal to the flow boundary and x and x' are the distances along the flow at corresponding points. The parameter H was postulated to depend on the nature of the polymer additive. This added complexity introduces the possibility that the best drag-reducing polymer might not necessarily be the best surface-pressure-fluctuation reducer.

An experimental determination of the effect of drag reducing polymers on surface pressure fluctuations on rough surfaces is reported here. A limited amount of data on surface pressure fluctuations from rough surfaces can be found in Refs. [7] and [12]. The work reported in these references was carried out in air and should correspond to the zero polymer additive concentration case reported here.

II. EXPERIMENTAL PROCEDURE

The surface pressure fluctuation measurements were made in a rotating cylinder test facility. The facility consists of a cylinder 1 ft in diameter and 1 ft long positioned to rotate axially in a cylindrical steel tank 6 ft in diameter and 6 ft deep (Fig. 1). The rotating cylinder was supported by a hollow stainless steel shaft which was in turn mounted in two water-lubricated rubber bearings. The bearing on the driven (upper) end of the shaft was mounted in a wooden frame separated from the tank. A "V" belt drive transmitted power from an electric motor drive. This system was necessary to reduce machinery noise enough that it could be neglected in most pressure measurements. (Background noise was measured at at least 10 db below any pressure intensity levels shown in this report.)

The top of the cylinder was submerged 2 ft below the water surface. The second rubber bearing and a circular plate were mounted immediately above the cylinder. The second bearing was lightly loaded and did not produce much noise; the circular plate prevented the introduction of air into the core of the vortex generated during high-speed motion. The supporting cross-arm for the bearing and plate also served to reduce the rotation of the fluid in the tank.

The rotating cylinder was constructed of synthetic wood material (Renwood) with 3-inch-thick walls. The ends were capped with 1/4-inch-thick circular brass disks and then with 45° synthetic wood cones. A hollow center section provided space for instruments. Measurements showed this construction to be free of mechanical resonance peaks in a measured background noise spectrum. The cylinder and end cones were finished with a heavy coat of epoxy paint, then machined to a 0.001 in. runout, dynamically balanced and waxed and polished to a high gloss for smooth surface tests.

Surface roughness was produced by spraying the surface with lacquer and dusting glass beads on the surface while the lacquer was still tacky. (Two sizes of roughness were used, 0.018 and 0.015 in. diameter.)

A set of strain gages was mounted on the drive shaft of the rotating cylinder and served to measure the total torque exerted by the fluid on

the cylinder and end cones. A second dynamometer mounted on a similar mechanical bearing and shaft assembly with only the end cones duplicated measured the total drag on end cones alone. The measured drag on the cylinder could thus be corrected for drag on the end cones to permit calculation of average shear.

The surrounding tank capacity was 1260 gallons. The tank was filled to a depth of 5.5 ft either directly from the municipal water supply or from the contents of the laboratory's water tunnel. (The municipal water supply is processed river water.) The water tunnel is equipped with an air separator and pressure control. These make possible the rapid removal of dissolved and free air from the test water to achieve the desired air concentration level in the tank water. The total air content of the water was measured with a Van Slyke apparatus. A low air content for the water was required to reduce cavitation on the roughness elements. A steam heat exchanger was also installed in the tank to permit adjustment or control of water temperature. The temperature was held at 70°F for most tests.

Polymer was added to the tank to the desired concentration. The solution of water and polymer was allowed to stand at least overnight to permit complete dissolving of the polymer and to reduce the viscoelastic effect which many investigators have reported with freshly mixed Polyox 301. Ten ppmw borax was added to the polymer solution in the most recent tests. It was found that this tended to extend the life of the polymer solution and improve consistency of measurements.

The fluctuating pressure on the surface of the rotating cylinder was measured by a flush-mounted hydrophone 1/8 inch in diameter obtained on loan from NSRDC and described in Ref. [13]. The signal from the hydrophone was amplified by a low-noise preamplifier mounted within the rotating cylinder before transmission to the remaining processing equipment through a slip-ring on the cylinder shaft. The rms pressure (broad band) was measured by a Ballantine 300 true rms voltmeter and the power spectrum by a Quan-tech frequency analyzer. The surface pressure hydrophone and preamplifier low-frequency "roll-off" began at 200 Hz (3 db point). Background noise measurements were made by recessing the hydrophone 0.020 in. and covering the surface of the mounting hole with a brass shim stock. This produced a small air cavity above the hydrophone which

acoustically isolated the hydrophone from surface pressure fluctuations. These measurements showed background levels to be at least 20 db below those measured with the cover removed.

Pressure fluctuations were measured on the surface of the cylinder as a function of frequency as the frequency analyzer slowly scanned the frequency range. The polymer concentration (Polyox 301) was increased by increments up to a maximum of 1000 ppmw. The speed range of the drum surface was increased by increments from 12 fps to near 60 fps. The occurrence of cavitation prevented data taking at higher speeds.

III. BOUNDARY LAYER CHARACTERISTICS

A flat plate is the usual reference body for the investigation of surface pressure fluctuations or the effect of polymers in water solution on drag. The rotating cylinder has a more complicated boundary layer than a flat plate, and so considerable effort is required to demonstrate the usefulness of this device in these investigations. The rotating cylinder's greatest merits are that independent average shear measurements can be made by means of a torque dynamometer and that it has a minimum of moving machinery which generates noise. The latter feature is essential when measuring radiated noise which may contribute to the high-frequency part of the surface pressure fluctuation.

The turbulent flow between concentric rotating cylinders has been described by Pai [14]. The velocity distribution arises from the motion of the cylinder and the ring-shaped vortex around the cylinder which transfers momentum to the flow near the boundary. Pai identified two regions (designated "A" and "B") in the flow as shown in Figs. 2 and 3. Although a much larger gap was used in the present investigation, dye tracer measurements have shown the conical ends give rise to two vortices which apparently stabilized two more vortices adjacent to the cylinder surface, much as in Pai's sketch. Pai's type "B" flow exists at the center of the cylinder where surface pressure fluctuations and velocity measurements were taken. The flow between 3 in. and 18 in. from the cylinder surface agreed with Pai's findings $UR = \text{Const.}$, where U is the tangential velocity at radius R from the center of the cylinder. Closer to

the rotating cylinder surface, the measured flow velocity followed a semi-logarithmic law. Type "A" flow (Fig. 3) exists near the ends of the cylinder. If an analogy is made with flow over a flat plate, type "A" flow may be said to correspond to an adverse pressure gradient and type "B" flow to a favorable pressure gradient. Examination of the semilogarithmic plot of velocity on Fig. 6 for pure water flow shows that the "wake region" ($y^+ > 10^4$) does have a form analogous to a flat plate with a favorable pressure gradient [Ref. 20].

A typical velocity profile is shown with natural scales in Fig. 4. The boundary layer thickness δ , the displacement thickness δ^* and the momentum thickness θ are also shown on the figure. The three boundary layer thicknesses were determined graphically as follows: The velocity profile was plotted as a function of distance on logarithmic paper and the slope "n" determined. The ratio of δ/δ^* and δ/θ can be expressed in terms of n. Repeated determinations of δ , δ^* , and θ were made by a planimeter until the above ratios were found. This procedure was necessary because the transition from a semilogarithmic profile to a $UR = \text{Const.}$ profile is very difficult to recognize as both types of profiles are very flat at the outer region of flow. The shape factor defined as δ^*/θ is shown in Fig. 5 from Ref. [20]. Present measurements from the rotating cylinder have been added. It can be noted that the added points fall below the faired line for zero pressure gradient on a flat plate. This is again in accord with observations suggesting that the rotating cylinder boundary layer is analogous to a favorable pressure gradient boundary layer in the central region of the rotating cylinder.

Fig. 6 shows several measurements of velocity profiles on the rotating cylinder presented on a semilogarithmic plot. The upward shift ΔB with the addition of polymer is nearly the same magnitude as occurs on a flat plate for the same effective concentration. (Maximum drag reduction for Polyox occurs in the region of 50 and 100 ppmw.) The downward shift with the addition of roughness and the shift back toward the smooth surface profile value with the addition of polymer are also apparent [17].

It thus can be argued that the "inner region" of the boundary layer on a rotating cylinder is very similar to that of the plane boundary layer

in that all the usual effects of roughness or polymer additive are present to approximately the same degree. The flattening of the profiles in the "outer region" is typical of a favorable pressure gradient. In the case of the rotating cylinder, the effect of a favorable pressure gradient is produced by the superimposed flow toward the central region. The solid lines are extensions of data from Ref. [18]. Drag measurements in this study correlate well with the data [16]. The values of K/R express the equivalent surface roughness necessary to give the drag measurement results of Ref. [16] where K is the equivalent diameter of roughness.

IV. BOUNDARY LAYER MEASUREMENTS

Table I gives the boundary layer parameters for several cylinder surface speeds and two surface conditions.

Figure 7 shows the drag coefficient C_d , calculated from the moments measured by the shaft dynamometer, as a function of Reynolds number based on cylinder radius. Correction was made for the drag of the conical ends by measuring torque exerted by the cones separately. The two flows described earlier as types "A" and "B" exist at various places on the cylinder surface, as do intermediate patterns. Each region can be expected to have a different drag coefficient. All these contributions are averaged into the moment measurements to obtain the average drag coefficient and the wall shear stress τ_0 . This raises some questions regarding the use of this average wall shear in place of the local shear in this report for correlating wall pressure fluctuations.

Figure 8 compares the dimensional plot of surface pressure fluctuation amplitude against frequency for a boundary layer developed on a rotating cylinder with the boundary layer at a specific point on a body of revolution which was propelled by buoyancy [3]. The free-stream velocity of both the rising body and the rotating cylinder was 62 fps. Each apparatus had a 1/8 in. surface-mounted hydrophone. It is assumed that the active areas of both hydrophones were equal to their diameters. It is curious that the two spectra match, even in small details.

V. BROAD BAND PRESSURE FLUCTUATIONS

The simplest measure of fluctuating pressure is the broad-band rms value (P'). The ratio P'/τ_0 as a function of cylinder Reynolds number for a variety of conditions is shown in Figs. 9 and 10. Figure 9 shows P'/τ_0 for smooth surfaces and Fig. 10 for rough surfaces. Comparison using the ratio P'/τ_0 shows that broad band surface pressure fluctuations, when compared on the basis of average shear, remain nearly constant with the addition of either drag reducing polymer or roughness to the surface. This indicates that the observable changes are largely due to changes in shear. There is a trend, however, toward higher values of P'/τ_0 with the addition of polymer.

VI. PRESSURE SPECTRA

Spectra of surface pressure fluctuations are frequently correlated on the basis of $\frac{4\phi(\omega)}{2 \rho V^3 \delta^*}$ vs. $\frac{\omega \delta^*}{V}$ where $\phi(\omega)$ is the mean square pressure per radian, ω is 2π times the frequency, ρ is the liquid density, δ^* is the boundary layer displacement thickness, and V is the cylinder surface velocity. It has been argued from dimensional considerations [in Ref. 5, for example] that the high frequency part of the pressure spectrum should be correlated on the basis of "inner law" parameters, while for the low frequency part δ^* might be appropriate. Examination of the data of a number of authors has shown correlation with δ^* over the entire frequency range when the change in δ^* was small. However, in Ref. [20] δ^* was changed considerably by imposing adverse and favorable pressure gradients. It appeared that the high frequency part of the spectrum might have been better correlated with a constant length scale, while the low frequency part might have been scaled with δ^* .

If the assumption is made that the high frequency part of the pressure spectrum arises from the "inner law" and sublayer regions, then it would not be expected that the high frequency part would be influenced by pressure gradients, as the "inner law" region of the boundary layer is not affected by pressure gradients. The overlap region of the velocity profile, however, reflects changes in δ^* , and thus some of the low frequency pressure fluctuations may arise in this region. Measured convection velocities of approximately 0.8 of the

free stream velocity [7] for the low frequency part of the spectrum give further evidence that this part of the spectrum is associated with the overlap region.

One of the more easily observed effects of polymer addition on roughness on boundary layers is a shift in the Y^+ vs. U^+ line as shown in Fig. 6. This gives strong evidence that the effect of polymer addition and roughness is limited to the inner law region.

In view of the above arguments, a constant length rather than δ^* will be used to correlate pressure spectrum data to show the influence of the combination of roughness and polymer addition. The most readily available length is R , the radius of the rotating cylinder. The justification for this choice is by analogy with pipe flow when the pipe diameter is used. The rotating cylinder has a feature in common with pipe flow in that the boundary layer thickness does not change in the direction of flow. In addition, the cylinder radius R was shown to be useful in correlating drag coefficient measurements ([16] and Fig. 7).

Figure 11 is a composite plot of 38 records taken on the smooth cylinder at 12 to 102 fps velocity over a one-year time span. The solid line is a least square fit to the coordinates. The data were taken from a previous study [18]. They were arbitrarily broken down into four sets and each set assigned a different symbol so that the teletype which produced the plot would superimpose symbols in the region of most frequent occurrence and produce the visual effect of a variable density of points.

Figures 12 and 13 show the effect of Polyox added to the water in various concentrations. A reduction in intensity is evident at all frequencies with the greatest reduction at low frequencies. Figure 14 shows the effect of extreme range in Polyox 301 concentration. Ten ppmw shows good reduction at low frequencies, while 1000 ppmw shows little effect.

Figure 15 shows the effect of roughness on surface pressure fluctuation as compared with a smooth surface. It appears that rough data are shifted upward over the entire range of frequencies with the greatest shift at low frequencies. It is believed that the change in slope at $\log \omega R/V > 2.5$ is due to radiated noise. Reference [5] has previously shown such a change in slope at high frequencies on a rotating cylinder and attributes this to radiated noise using dimensional reasoning. Preliminary measurements of radiated noise from the cylinder with the same roughness showing a value of radiated noise intensity of nearly the same level as the

surface pressure fluctuations at a frequency of 3 Kilo-Hertz which corresponds roughly to $\log \omega R/V \approx 2.5$. This radiated noise is much reduced by the addition of polymer. Examination of surface pressure fluctuation intensities with polymer added to the fluid shows less of this change in slope at high frequencies.

No correction has been made for hydrophone size. Corcos [8] has given such a correction. However, its strict application would require information on the spatial correlation functions appropriate to the addition of roughness or polymer. Alternatively a calibration correction could be obtained using a number of sizes of hydrophones [19].

Fig. 16 presents a comparison of the pressure fluctuation intensity as the surface friction is increased from that of a smooth surface by roughness or reduced by the addition of a polymer to the fluid.

The effect of various concentrations of polymer additive on pressure fluctuations on rough surfaces is shown in Fig. 17. A reduction of approximately 10 db is evident in the low-frequency range for polymer concentrations of 50 ppmw and greater. Little reduction in pressure fluctuations is evident in the mid-frequency range. It has already been argued that the observable reduction at high frequencies is in the radiated component of flow noise.

The presence of roughness on the surface raises the question of the influence of the location of roughness elements with respect to the hydrophone base on the level of measured intensity. It is conceivable that roughness elements on the hydrophone surface could induce a moment due to shear which would appear as a pressure signature. Data were taken on the rough surface, with roughness on the hydrophone, with roughness off the hydrophone surface only, and with smooth areas of $3/8$ and $3/4$ in. diameter around the hydrophone. These results, shown in Fig. 18, indicate little difference except for that due to scatter. A tentative conclusion is that any smooth area around the hydrophone less than one displacement thickness in radius gives substantially the same result. The clear area at its maximum in this case was 0.37 in. in radius and δ^* was approximately 0.8 inches. Since results did not seem sensitive to clear areas around the hydrophone, further data were taken with only the hydrophone surface free of roughness.

Figure 19 shows a further check on the influence of roughness location with respect to the hydrophone face when influenced by the presence of polymer. Three conditions are shown: a $3/4$ -in.-diameter smooth area around the hydrophone, a $3/8$ -in.-diameter smooth area around the hydrophone, and roughness off the face of the hydrophone only. A Polyox concentration of 100 ppmw was used. The result for roughness element off the hydrophone surface only lies between the result for the $3/8$ -in.-diameter smooth area around the hydrophone and that for the $3/4$ -in.-diameter smooth area around the hydrophone. The most reasonable interpretation is that this is a random effect rather than a systematic effect which is dependent on the diameter of the smooth area. As was previously observed in water only, the smooth area around the hydrophone has little effect in the presence of polymer additive. No doubt a smooth area diameter exists for which the surface fluctuations observed would become comparable to those of a smooth surface. However, experimental conditions were too restricted to show this limit.

Some of the data of Figs. 11 through 17 are replotted in Figs. 20 through 22 introducing C_d as defined in Fig. 7 to the ordinate scale. This form of plotting is intended to show the influence of fluid friction on the various pressure fluctuation spectra. The solid lines in each graph are least square fits from the coordinates of each data point.

Figure 20, for runs with water only on a smooth surface, is typical of the scatter of the data as compared to the fitted line. It can be compared with the same data plotted in Fig. 11. In addition, a few representative points from data of Schloemer [20] are shown for comparison. These points have been superimposed by replacing Schloemer's boundary layer thickness with the radius of the cylinder used in this experimental work. Either the match of the data for a zero pressure gradient must be regarded as coincidental or it must be assumed that a common turbulence length parameter is present in both experimental conditions.

Schloemer also presented data obtained on a smooth boundary with a variable pressure gradient. The favorable pressure gradient produced a thinner displacement thickness and an increased drag coefficient, while the adverse pressure gradient increased the displacement thickness and

reduced the drag coefficient as compared to the zero pressure gradient case. This is in general in contrast with the effects of polymer additive, which give a thinner displacement thickness and lower surface friction, or of roughness, which give a large displacement thickness and greater surface friction. This is reflected also by the failure of the drag coefficient to correlate with the pressure fluctuation at low frequencies, particularly for the favorable pressure gradient. If Schloemer's adverse pressure gradient data points in Fig. 20 are compared with the fitted curve for a smooth surface with Polyox shown on Fig. 22, considerable agreement is apparent. It was mentioned earlier that both adverse pressure gradient and polymer produced a similar reduction in drag coefficient.

In Fig. 21 data for rough surfaces, rough surfaces with polymer additive, and smooth surfaces with polymer additive are plotted on the same coordinates as were used in Fig. 20. Representative points from rough surface boundary layers as measured by Blake [7] are shown for comparison. The points were again fitted as in the previous graph by replacing Blake's measured displacement thickness with the cylinder radius. Blake's experiments were performed in air with greater roughness than that used in the work reported here. A sufficiently small sensor was used by Blake to eliminate the necessity of a size correction.

Figure 22 shows the fitted lines from the four experimental conditions, smooth and rough surface with and without drag reducing polymer additives, to allow comparison of these four different surface friction conditions as reflected by the surface friction pressure intensity. Some differences in detail are evident. At values of $\log \frac{\omega R}{V}$ between 1 and 2, there appears to be a greater reduction in drag coefficient than in pressure fluctuation with the addition of polymer and, conversely, a greater increase in surface pressure fluctuation than in drag coefficient with addition of roughness. Reduction in surface pressure fluctuation for values of $\log \frac{\omega R}{V}$ between 2 and 3 appeared to be greater than the reduction in drag coefficient with polymer additions on rough surfaces. The fitted curves seem to come together for values of $\log \frac{\omega R}{V} < 1$. The upward bend at the extreme left, however, is of no significance, since it is the result of extending the curve equation slightly beyond the data.

It is likely that a correction for hydrophone size will reduce the spread of data in the region of $1 < \log \frac{\omega R}{V} < 2$ and that a correction for radiated noise from rough surfaces will reduce the spread of data at high frequencies ($R > 2$). The data appear to correlate well below $\log \frac{\omega R}{V} = 1$, which is the region expected to require no correction for sensor size [8].

VII. SUMMARY

It appears from the data presented that the intensity of surface pressure fluctuation correlates well on the basis of $\frac{4\phi(\omega)}{2^3 V^3 R}$ vs. $\log \frac{\omega R}{V}$ where the cylinder radius R has been substituted for the more traditional displacement thickness (δ^*).

When the turbulent surface friction is altered from a smooth surface value by the addition of roughness to the surface or of drag-reducing polymer to the test liquid, or both, the resulting change appears to be, on the average, proportional to the change in the square of the average surface drag coefficient.

Experiments with roughness elements placed up to $3/8$ in. from a $1/8$ -in. surface pressure sensor center ($3/4$ -inch-diameter smooth circle) show little difference from measurements obtained with roughness elements at the edge of the sensor.

It has been suggested by Black [6] that the surface pressure fluctuation intensity might be a means of inferring local shear. The results shown in Fig. 22 indicate that shear might be inferred for a wide range of conditions of roughness and of polymer additive concentration if the pressure intensity spectrum frequency range is suitably chosen.

The following tentative observation might be made based on the data presented here and the limited data taken from other experimenters. The data have been correlated on a constant length parameter basis (R , the radius of the cylinder, was used, replacing the more widely used boundary layer displacement thickness δ^*). The drag coefficient C_d was also included in the correlation in order to account for changes in surface drag produced by changes in roughness or the addition of a drag reducing polymer.

These parameters were shown to be adequate so long as the displacement thickness was directly related to the drag coefficient, as in the case of a flat plate with a zero pressure gradient or a pipe.

If one writes the momentum equation for the boundary layer [21],

$$\frac{\partial \theta}{\partial x} = \frac{(H + 2)}{2} \frac{\theta}{\frac{\rho U^2}{2}} \frac{\partial P}{\partial x} + C_d$$

it is apparent that the relationship between drag and displacement thickness (related to θ by H) becomes more involved in the presence of a pressure gradient. The low-frequency pressure fluctuations are, nevertheless, closely related to the displacement thickness δ^* [20]. The high-frequency spectral region also appears to be related by the surface friction to a constant length parameter, as in the zero-pressure-gradient case.

The adoption of the cylinder radius R as constant length parameter in this investigation was rather arbitrary. From observations of shear measurements by hot-film surface probes, evidence is available of a constant wave number based on a convection velocity and sublayer periodicity [22] which, if better understood, would possibly serve as a replacement for R .

It has been proposed that the highest frequency part of the data, $2 < \frac{\omega R}{U} < 3$, shows the presence of radiated noise.

REFERENCES

- [1] Skudrzyk, E. and Haddle, G., "The Physics of Flow Noise," Journal of Acoustical Society of America, Vol. 40, No. 1, Part 2, January 1969, pp. 130-157.
- [2] Skudrzyk, E. and Haddle, G., "Noise Production in a Turbulent Boundary Layer by Smooth and Rough Surface," Second Symposium on Naval Hydrodynamics, 1958, pp. 75-103.
- [3] Nisewanger, C. R. and Sperling, F. B., Flow Noise Inside Boundary Layer of Buoyancy Propelled Test Vehicles, Technical Paper 3511, Naval Ordnance Test Station, April 1965.
- [4] Wetzel, J. M.; Almo, J. A.; and Killen, J. M., "Turbulence Measurements in Dilute Polymer Flows," Symposium on Turbulence Measurement, University of Missouri, Rolla, September 1969.
- [5] Foxwell, J. H., The Wall Spectrum Under a Turbulent Boundary Layer, AUWE Tech. Note 218/66, Admiralty Weapons Establishment, Portland, 1966.
- [6] Black, T. J., Some Practical Applications of a New Theory of Wall Turbulence, Tracor, Inc., Rockville, Maryland, 1967.
- [7] Blake, W. K., "Turbulent Boundary Wall Pressure Fluctuations on Smooth and Rough Wall," Journal of Fluid Mechanics, Vol. 44, Part 4, December 1970, pp. 637-660.
- [8] Corcos, G. M., "Resolution of Pressure in Turbulence," Journal of Acoustical Society of America, Vol. 35, 1963, pp. 192-199.
- [9] Heaps, H. S., "Effect of Turbulence Nearfield on a Shielded Transducer," Journal of Acoustical Society of America, Vol. 40, No. 6, 1966, pp. 1331-1336.
- [10] Meyers, W. A., "A Correlation of the Frictional Characteristics for Turbulent Flow of Dilute Viscoelastic Non-Newtonian Fluid in Pipes," AIChE Journal, Vol. 12, 1966, pp. 522-525.
- [11] White, F. M., "An Analysis of the Effect of Polymer Additives on Boundary Layer Noise," AIAA Paper No. 68-642, AIAA 4th Propulsion Joint Specialist Conference, June 1968.
- [12] Hennen, H. A., Miniature Piezoelectric Transducers for Broad-Band Noise Measurements, M.S. thesis, University of Minnesota, March 1968.
- [13] Franz, G. J., "Flow Measurements in Water," 72nd Meeting of the Acoustical Society of America, November 2-5, 1968.
- [14] Pai, Shih-I., Turbulent Flow Between Rotating Cylinders, NACA Technical Note 893, March 1943.

- [15] Virk, P. S.; Mickley, H. S.; and Smith, K. A., "The Ultimate Asymptote and Mean Flow Structure in Toms Phenomenon," Transactions, ASME, June 1970, pp. 488-493.
- [16] Theodorsen, T. and Regier, A., Experiments on Drag of Revolving Disks, Cylinders, and Streamlined Rods at High Speeds, NACA Report 793, 1944.
- [17] Spangler, J. G., "Studies of Viscous Drag Reduction with Polymers Including Turbulence Measurements and Roughness Effects," Viscous Drag Reduction, C. S. Wells, Ed., Plenum Press, 1969, pp. 131-158.
- [18] Killen, J. M. and Almo, J. A., "An Experimental Study of the Effect of Dilute Solutions of Polymer Additive on Boundary Layer Characteristics," Viscous Drag Reduction, C. S. Wells, Ed., Plenum Press, 1969, pp. 447-461.
- [19] Geib, F. E., Jr., "Measurements of the Effects of Transducer Size on the Resolution of Boundary Layer Pressure Fluctuations," Journal of Acoustical Society of America, Vol. 46, No. 1, Part 2, July 1969, pp. 253-261.
- [20] Schloemer, H. H., Effects of Pressure Gradients on Turbulent Boundary Layer Wall-Pressure Fluctuations, Report No. 747, U.S. Underwater Sound Laboratory, Fort Trumbull, New London, Connecticut, July 1966.
- [21] Schubauer, G. B. and Tchen, C. M., Turbulent Flow, C. P. Donaldson, Ed., Princeton University Press, Princeton, New Jersey, 1961.
- [22] Geremia, J. O., An Experimental Investigation of Turbulence Effects at the Solid Boundary Using Flush Mounted Hot Film Sensor, Ph.D. dissertation, George Washington University, Washington, D. C., January 1970.

T A B L E IMean Properties of Flow Boundary Layers

TABLE I -- Mean Properties of Flow Boundary Layers

Type	Cylinder Velocity V, fps	Particle Diam. K, in.	K Equiv- alent, in.	δ_{99} , in.	δ^* , in.	θ , in.	H	C_d	U* fps	Cylinder Radius Reynolds Number	Momentum Thickness Reynolds Number
Tap water											
Smooth surface	25.1	--	--	3.4	.24	.232	1.18	.00231	.885	1.19×10^6	4.8×10^4
50 ppmw + water											
Polyox 301											
Smooth surface	25.1	--	--	3.4	.21	.184	1.13	.00107	.59	1.19×10^6	3.84×10^4
Tap water											
Smooth surface	38.0	--	--	2.68	.223	.188	1.18	.00236		1.79×10^6	7.1×10^4
Water + 50 ppmw											
Polyox 301											
Smooth surface	38.0	--	--	2.9	.151	.14	1.11	.00228	.835	1.79×10^6	4.42×10^4
100 ppm Polyox 301											
Rough surface R70	19.0	.018	0.0034	8.1	.418	.384	1.09	.0038	.83	8.94×10^5	6.1×10^4
Tap water											
Rough surface R70	19.0	.018	0.032	9.9	.79	.684	1.16	.0065	1.08	8.94×10^5	1.08×10^5
Tap water											
Rough surface R70	25.0	.018	0.032	14.5	.75	.668	1.12	.0074	--	1.19×10^6	1.39×10^5
100 ppmw Polyox 301											
Rough surface R70	25.0	.018	0.034	11.5	.48	.444	1.09	.0041	1.52	1.19×10^6	9.15×10^4
Tap water											
Rough surface R70	12.0	.018	0.032	11.8	.63	.568	1.11	.0071	.716	5.96×10^6	5.68×10^4
100 wppm Polyox 301											
Rough surface R70	12.0	.018	0.0034	10.0	.545	.48	1.11	.0038	.524	5.96×10^6	4.8×10^4
Tap water											
Rough surface	31.0	.018	0.032	9.8	.666	.58	1.15	.0078	1.93	1.49×10^6	1.49×10^4
100 ppmw Polyox 301											
Rough surface R70	31.0	.018	0.0034	8.2	.423	.38	1.11	.0052	1.54	1.49×10^6	9.8×10^4
Water only											
Rough surface	19.0	.015	0.019	--	--	--	--	.006	1.07	8.94×10^5	--
25 ppmw Polyox 301											
Rough surface	19.0	.015	0.0044	--	--	--	--	.004	.98	8.94×10^5	--

F I G U R E S
(1 through 22)

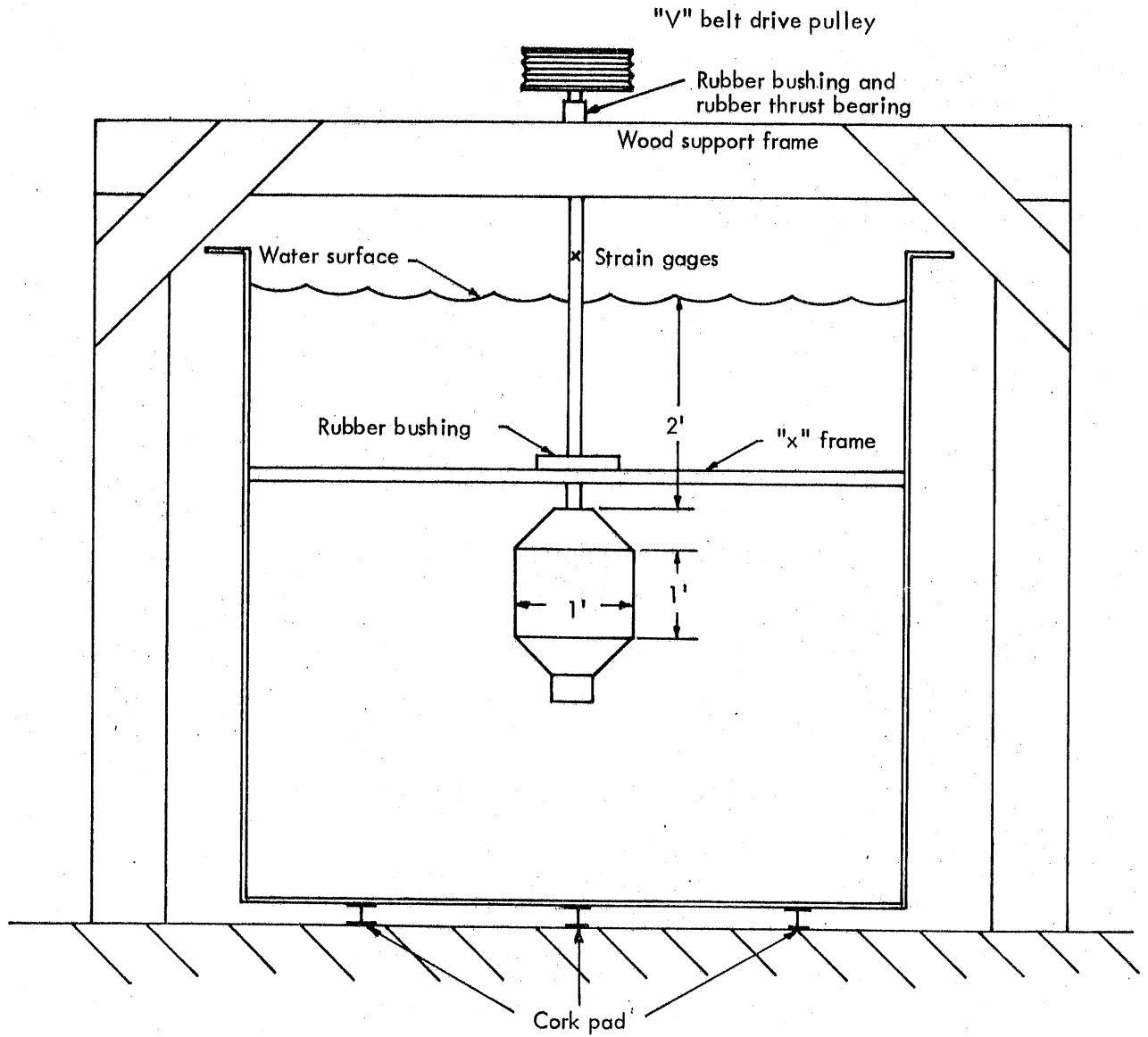


Fig. 1 - Sketch of Test Tank with Rotating Cylinder in Place

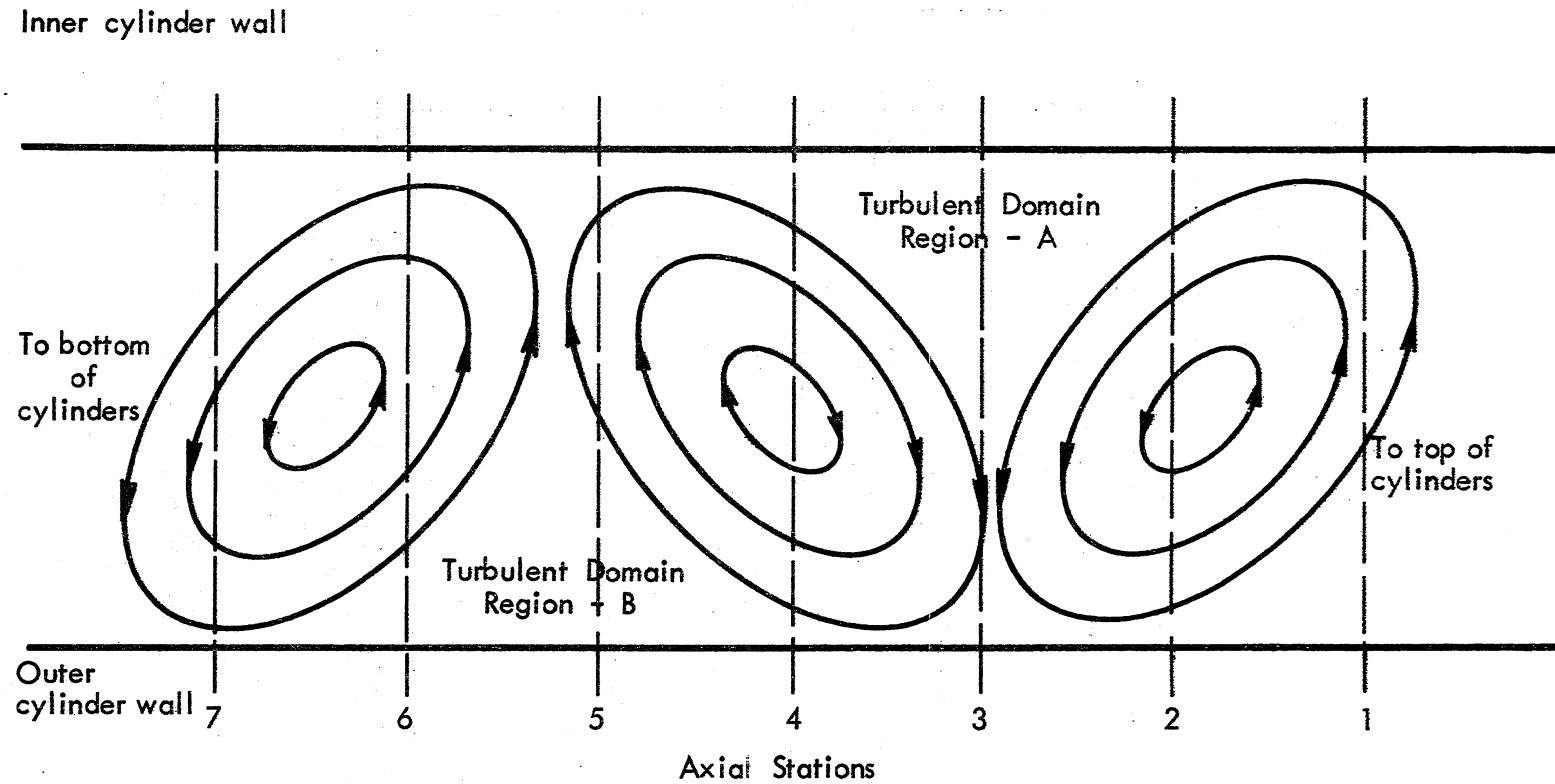


Fig. 2 - Vortices between Rotating Cylinders
(Ref. [14])

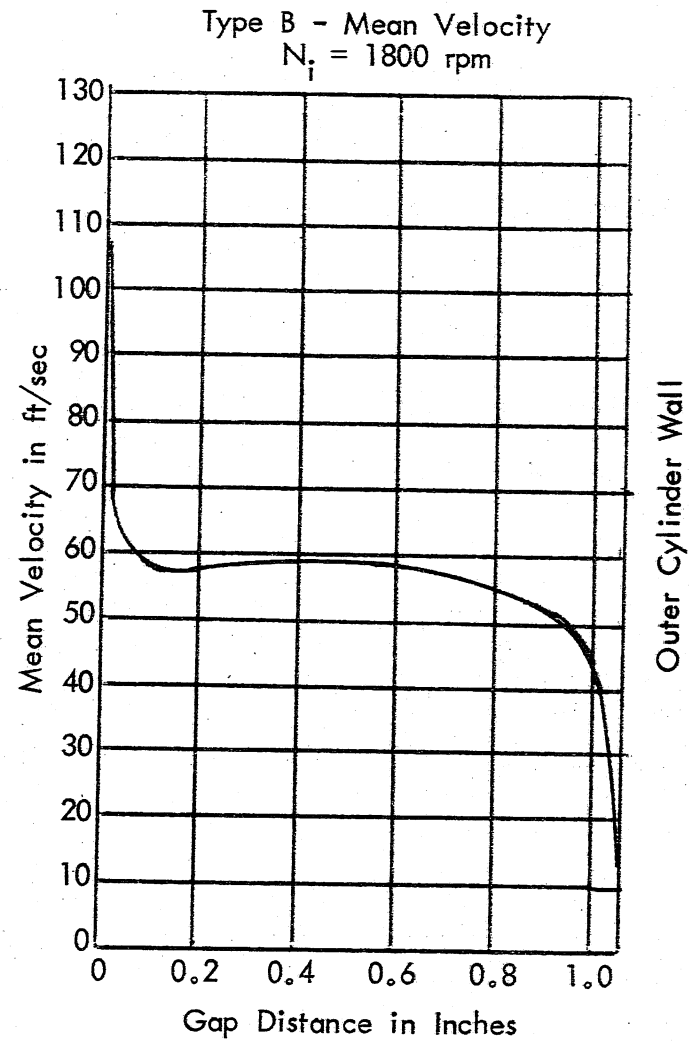
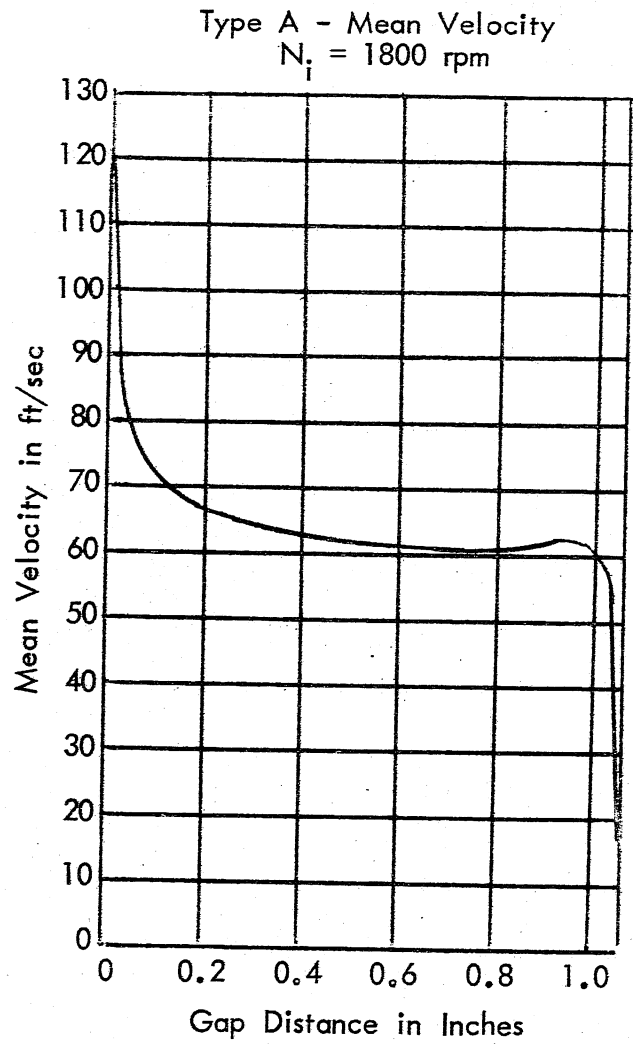


Fig. 3 - Mean Velocity Distribution for Type A and Type B Flow (Ref. [14])

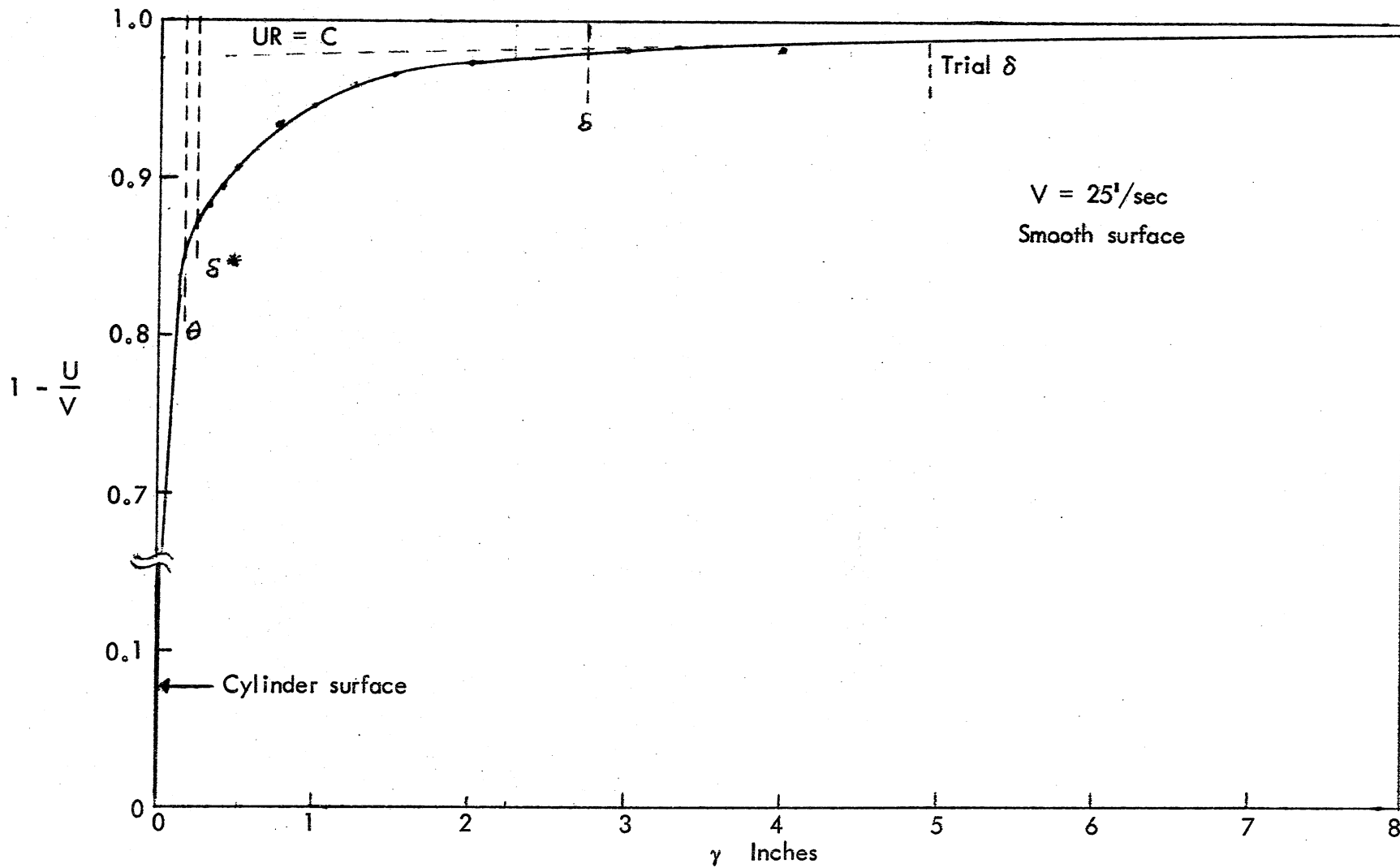


Fig. 4 - Typical Velocity Profile

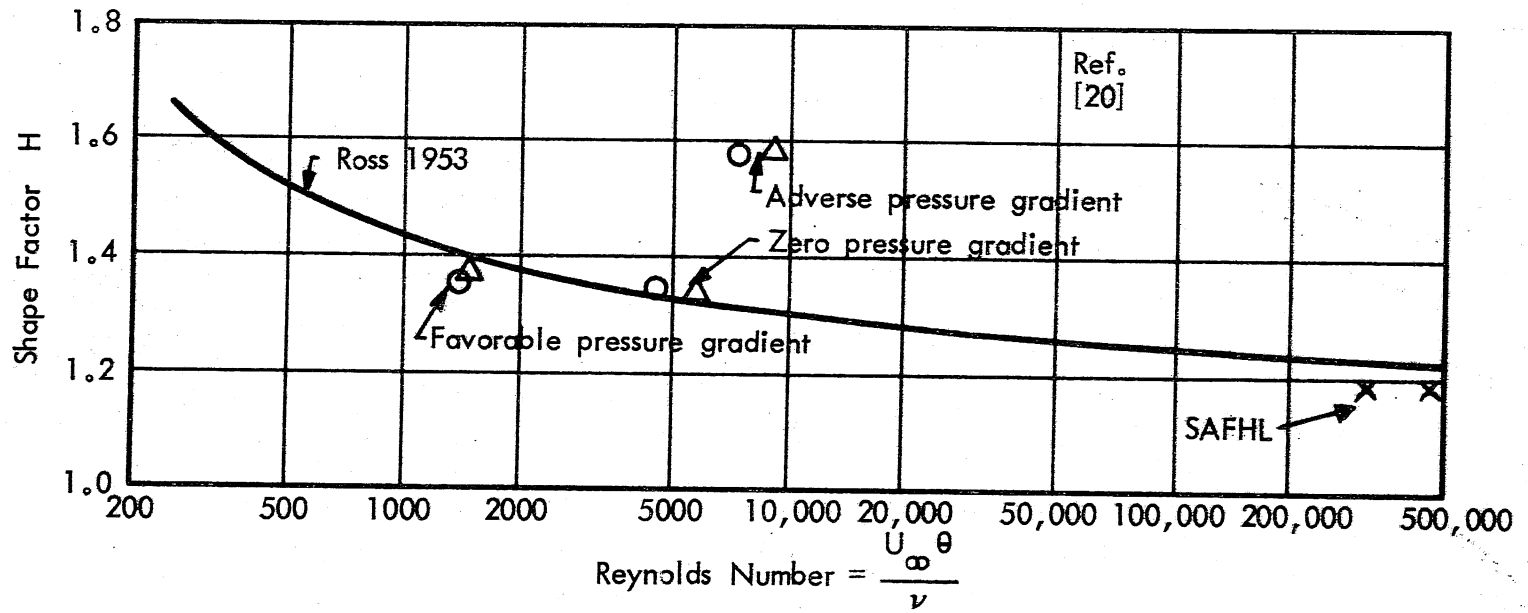


Fig. 5 - Shape Factor vs. Reynolds Number

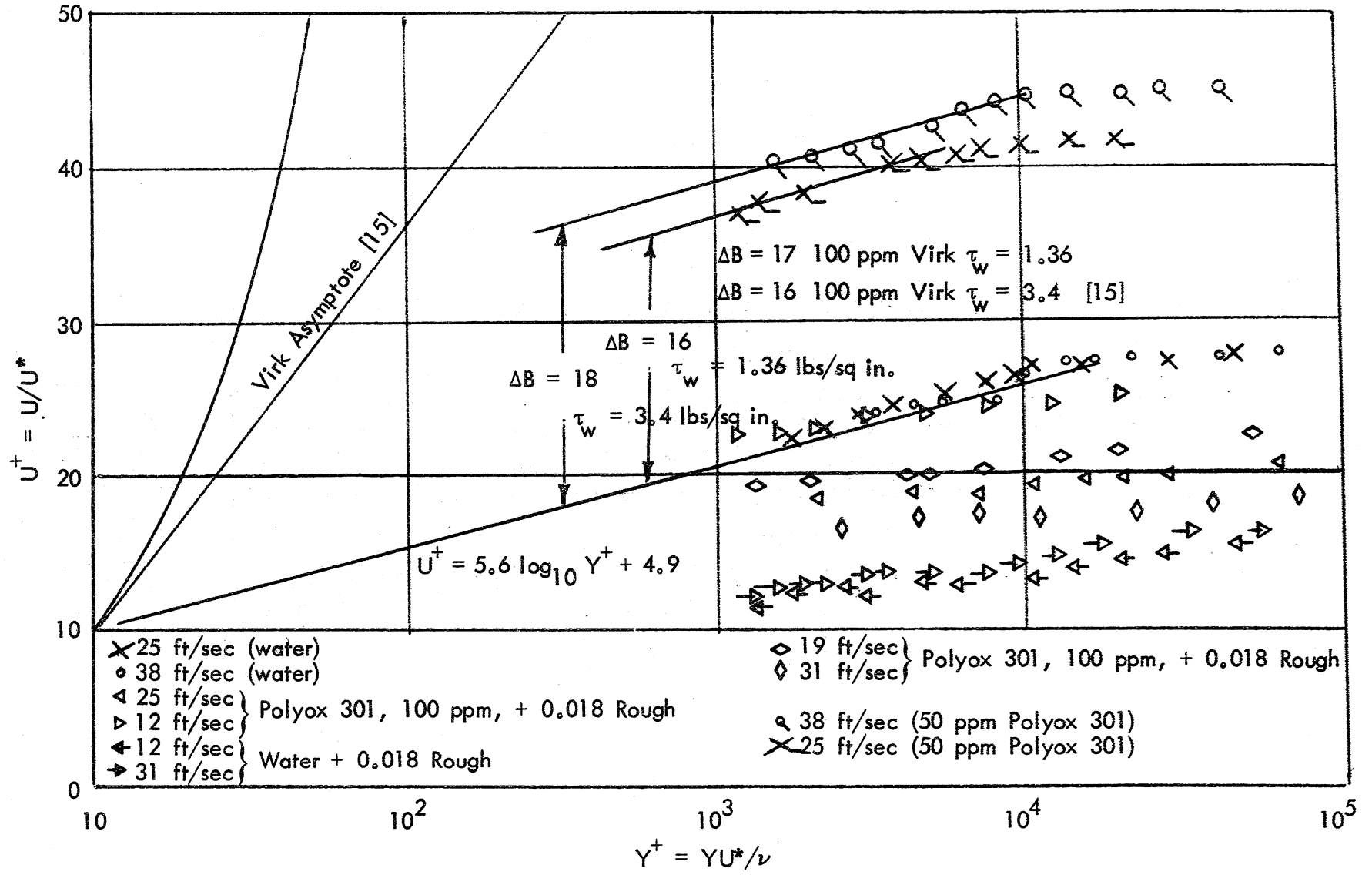


Fig. 6 - Velocity Profile near Rotating Cylinder

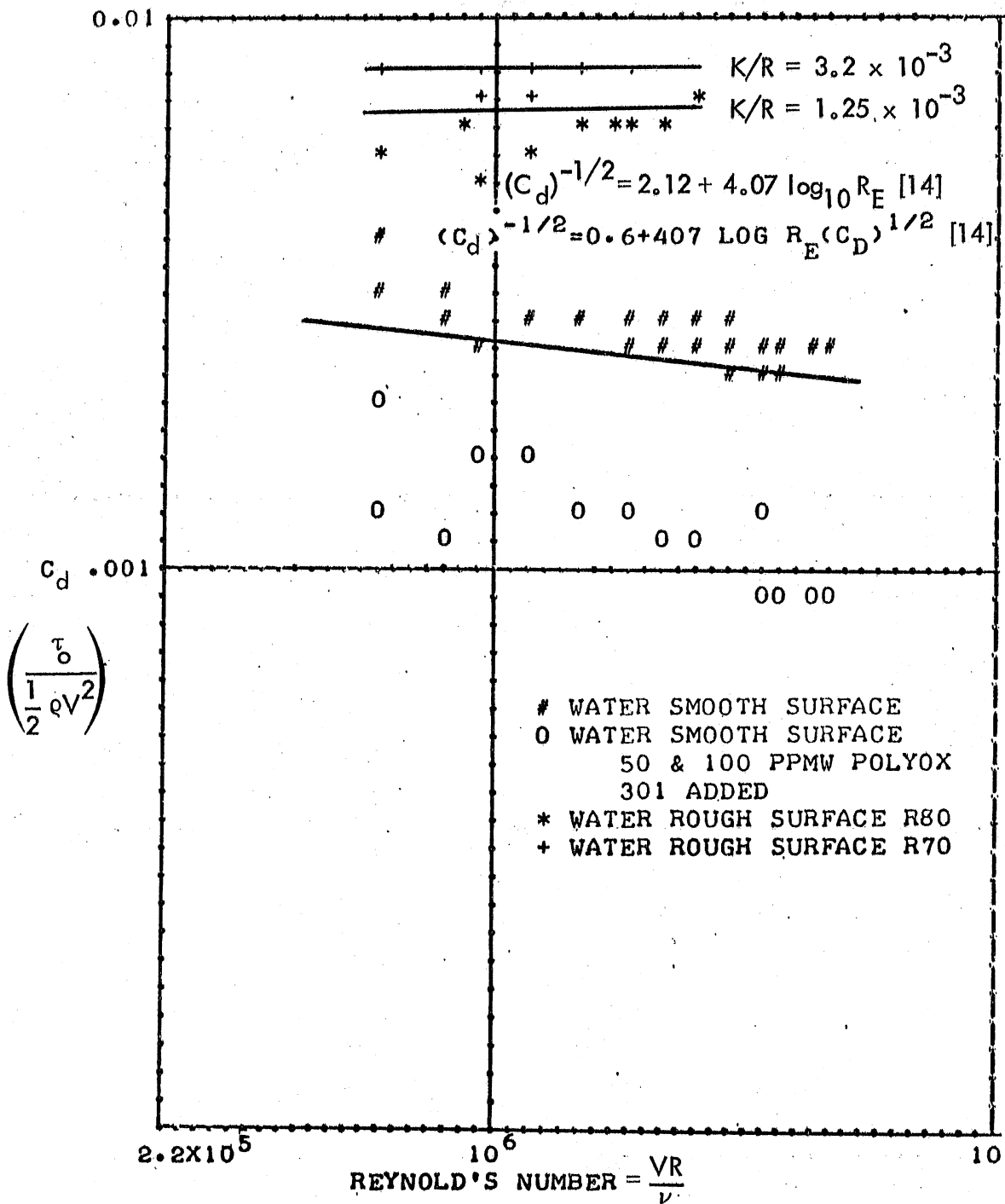


Fig. 7 - Measured Cylinder Drag Coefficient

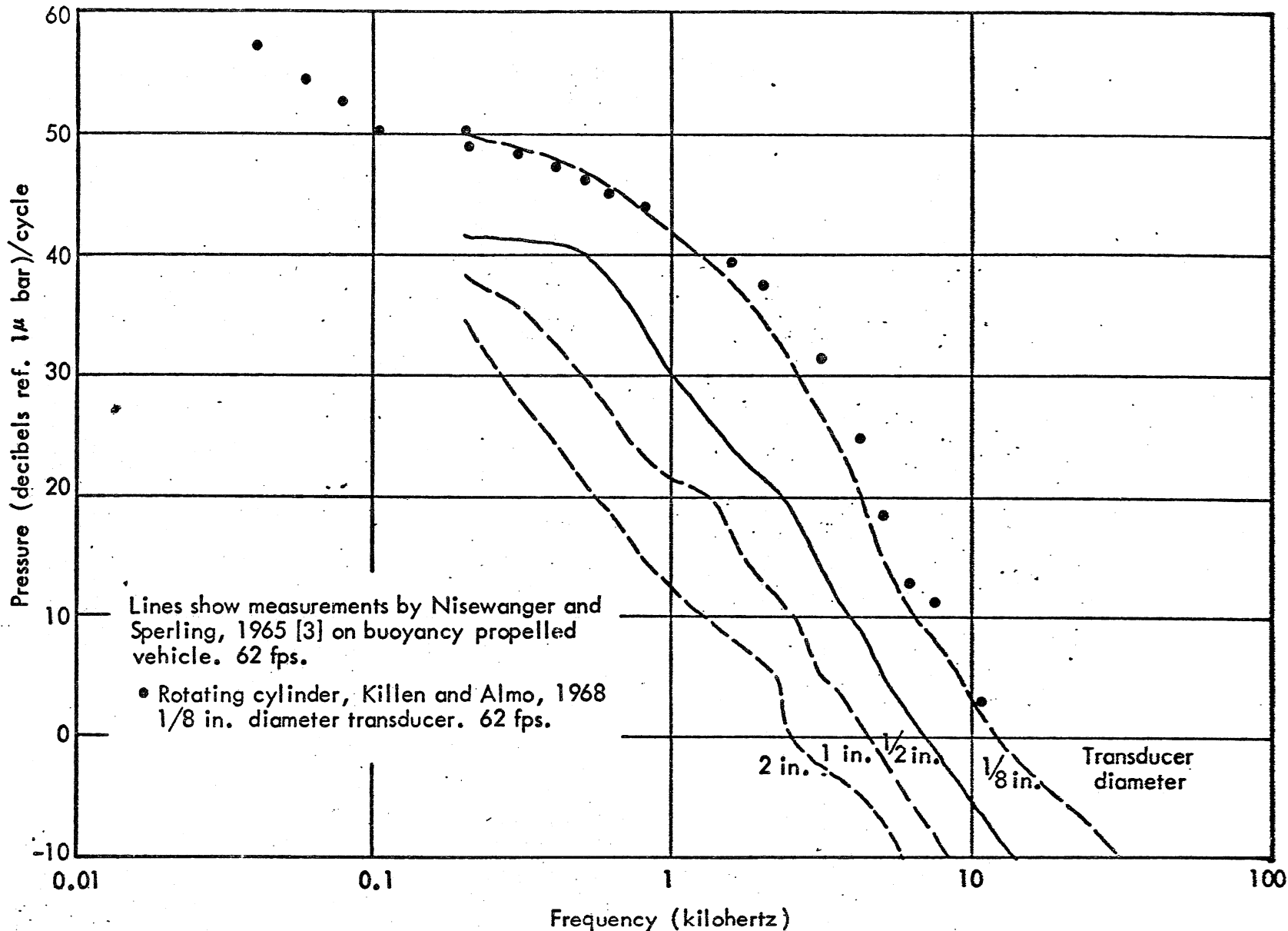


Fig. 8 - Comparison of Surface Pressure Fluctuation on a Rotating Cylinder and Buoyant Body

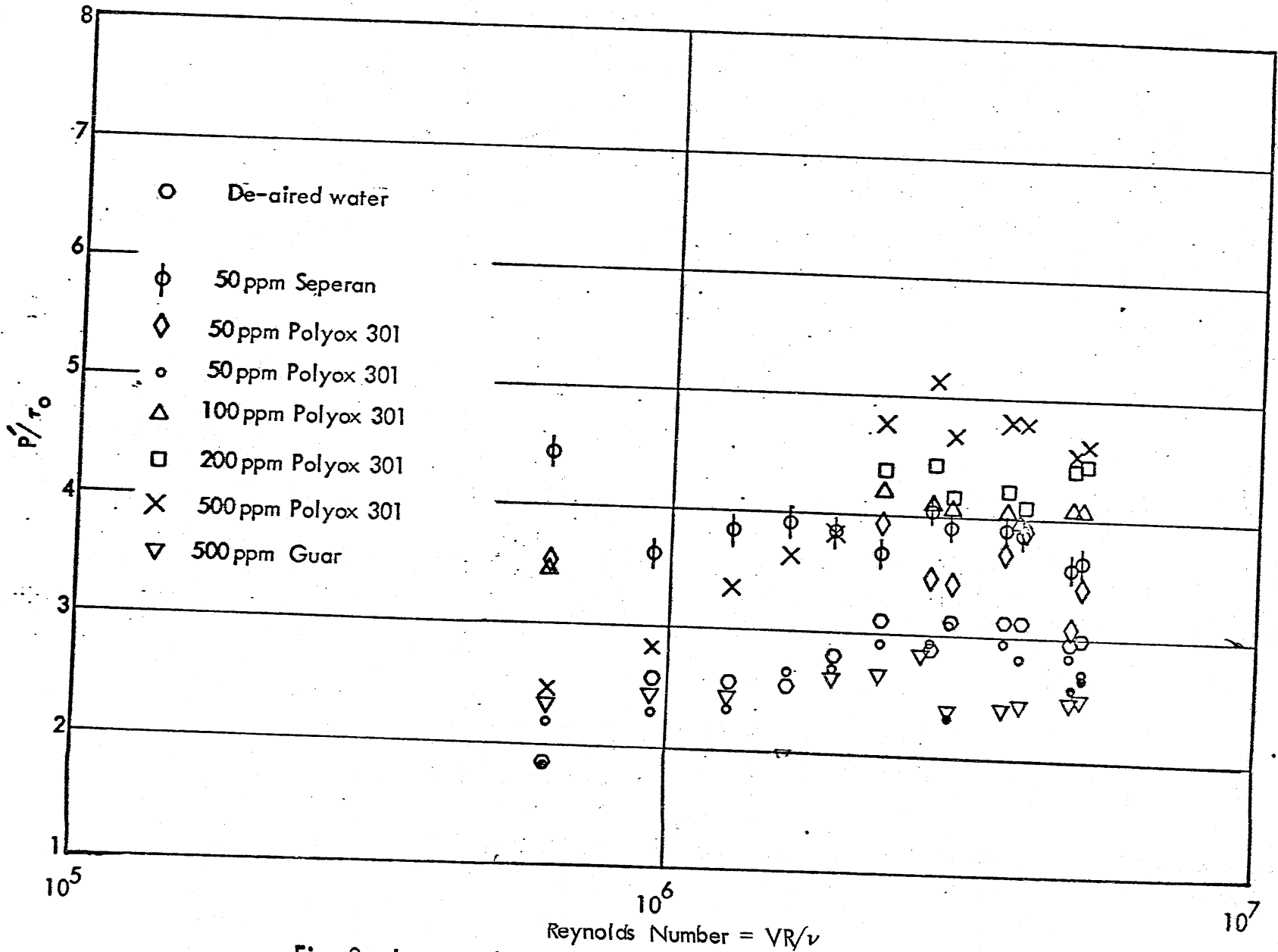


Fig. 9 - Integrated Root-Mean Square Surface Pressure Fluctuation on a Smooth Surface

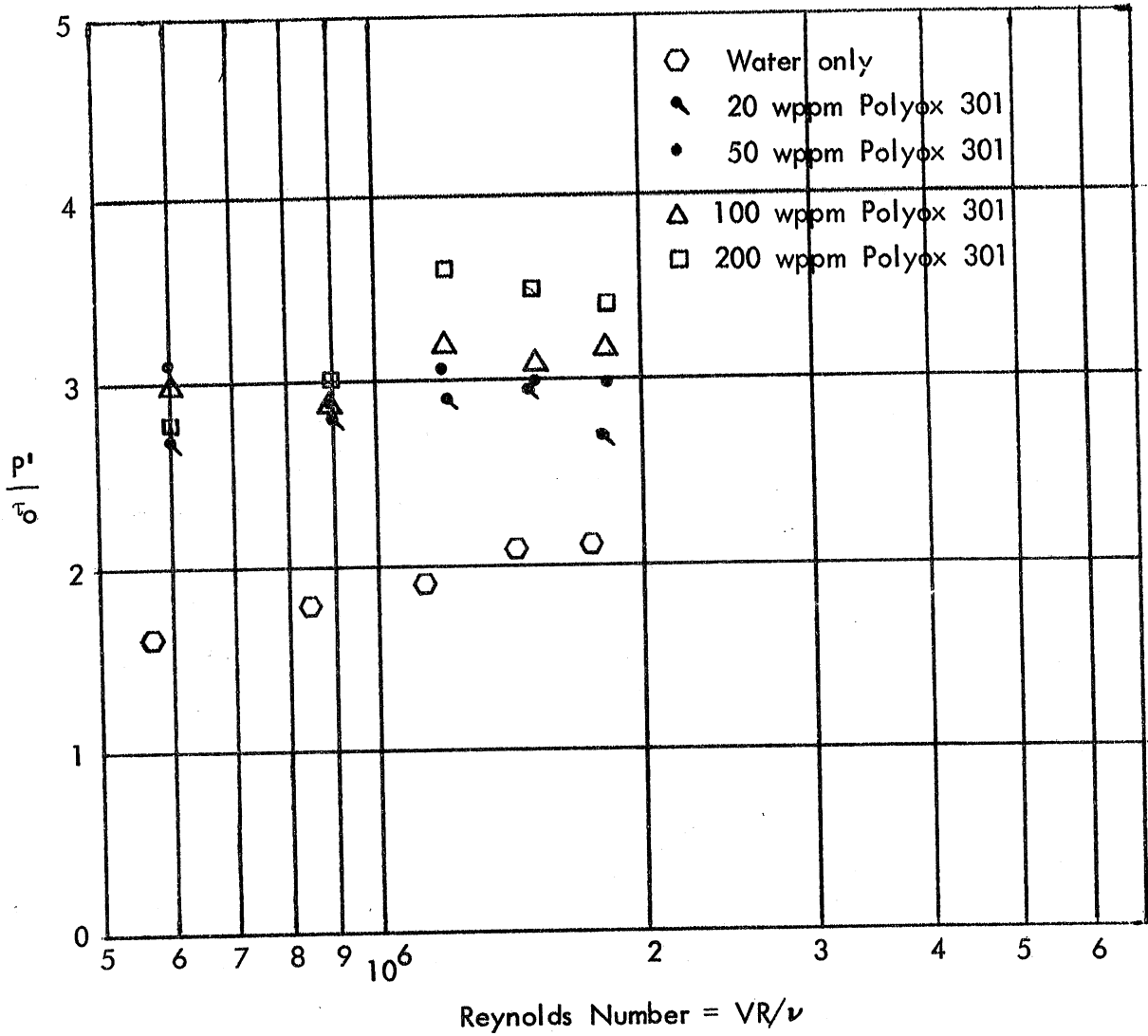


Fig. 10 - Integrated Root Mean Square Surface Pressure Fluctuation on a Rough Surface (0.018 in. diam. bead roughness, 1/8 in. diam. hydrophone, smooth surface)

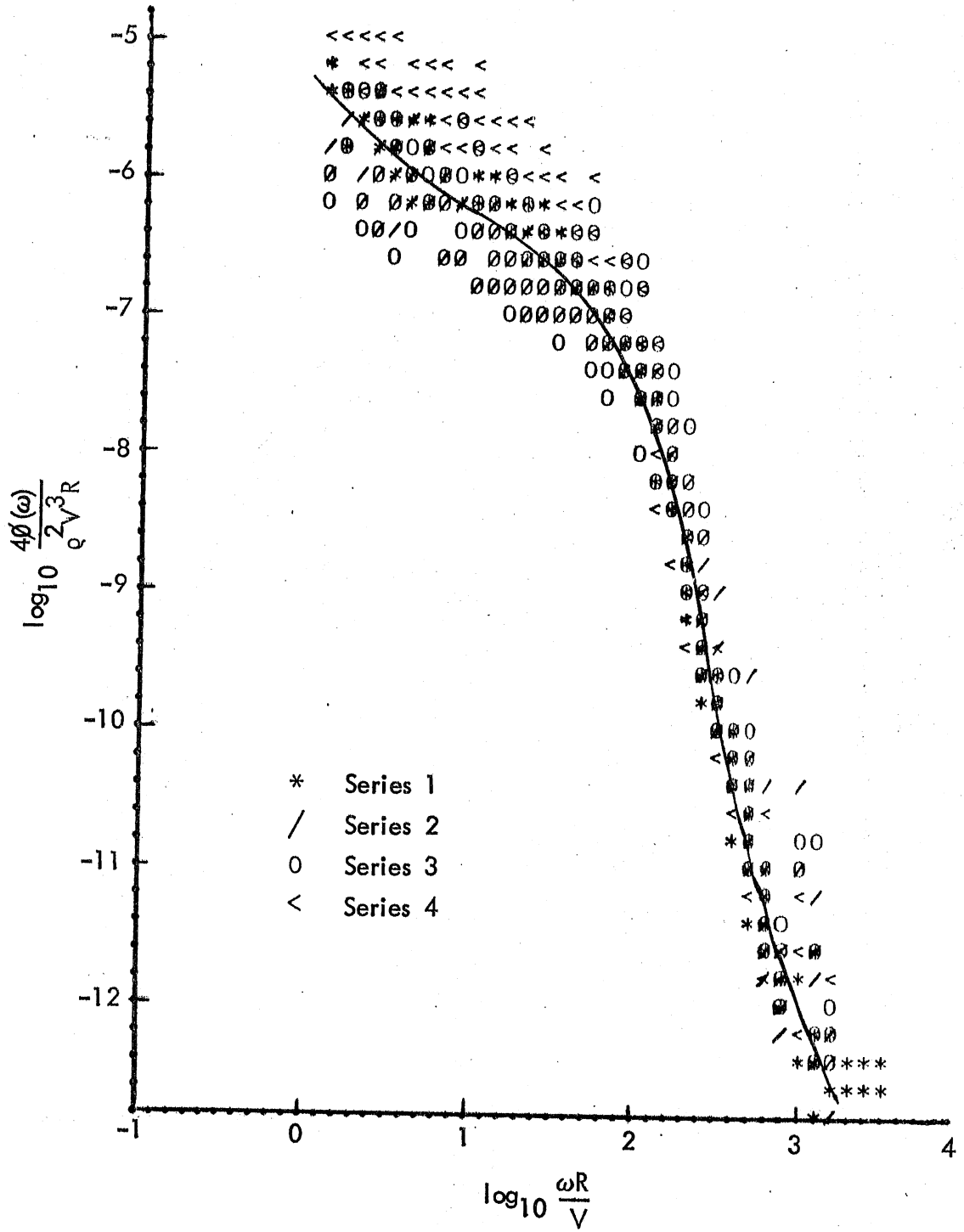


Fig. 11 - Surface Pressure Fluctuation Spectra in Water on a Smooth Surface

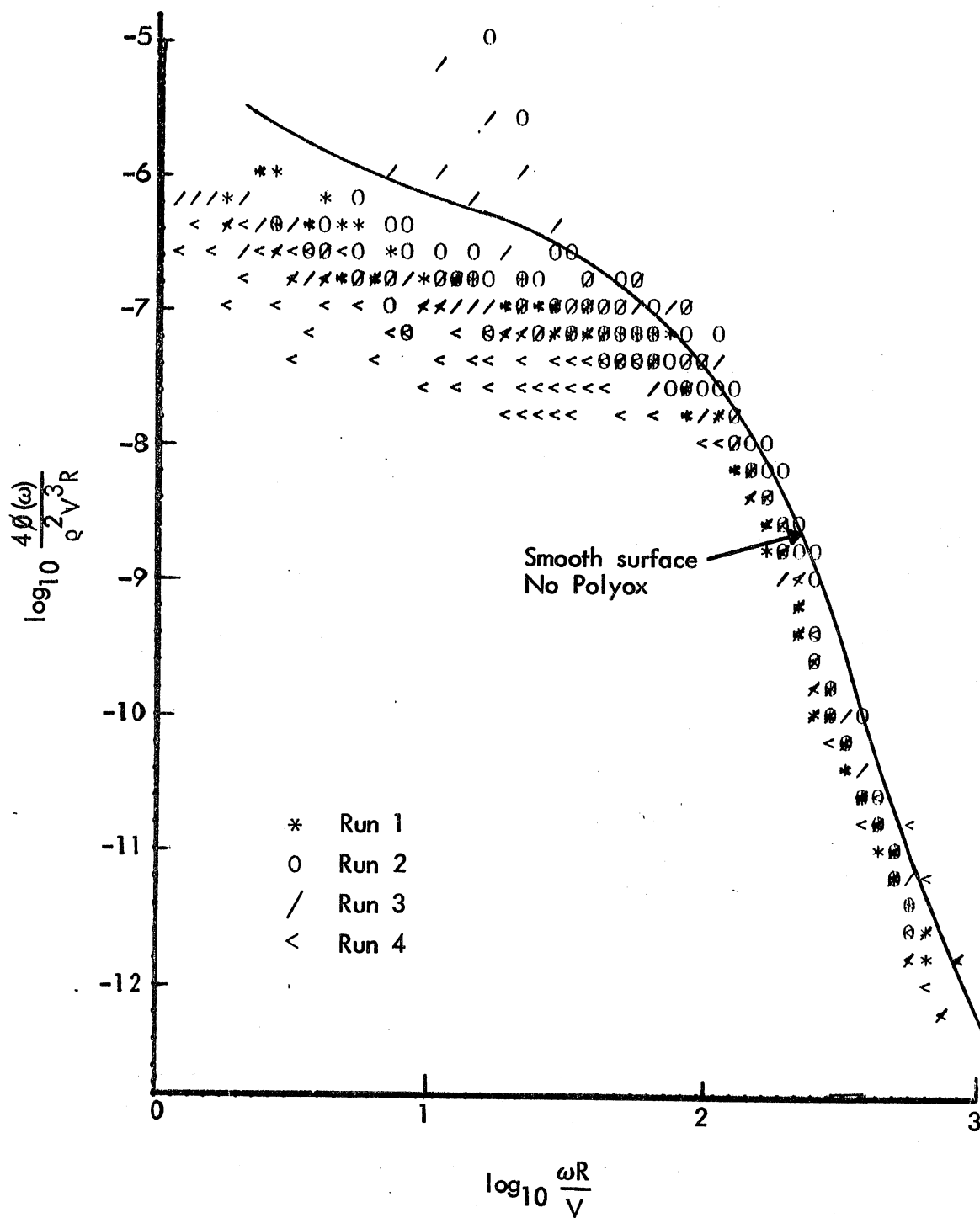


Fig. 12 - Surface Pressure Fluctuation Spectra on a Smooth Surface with 50 ppmw Polyox 301 added to the Water

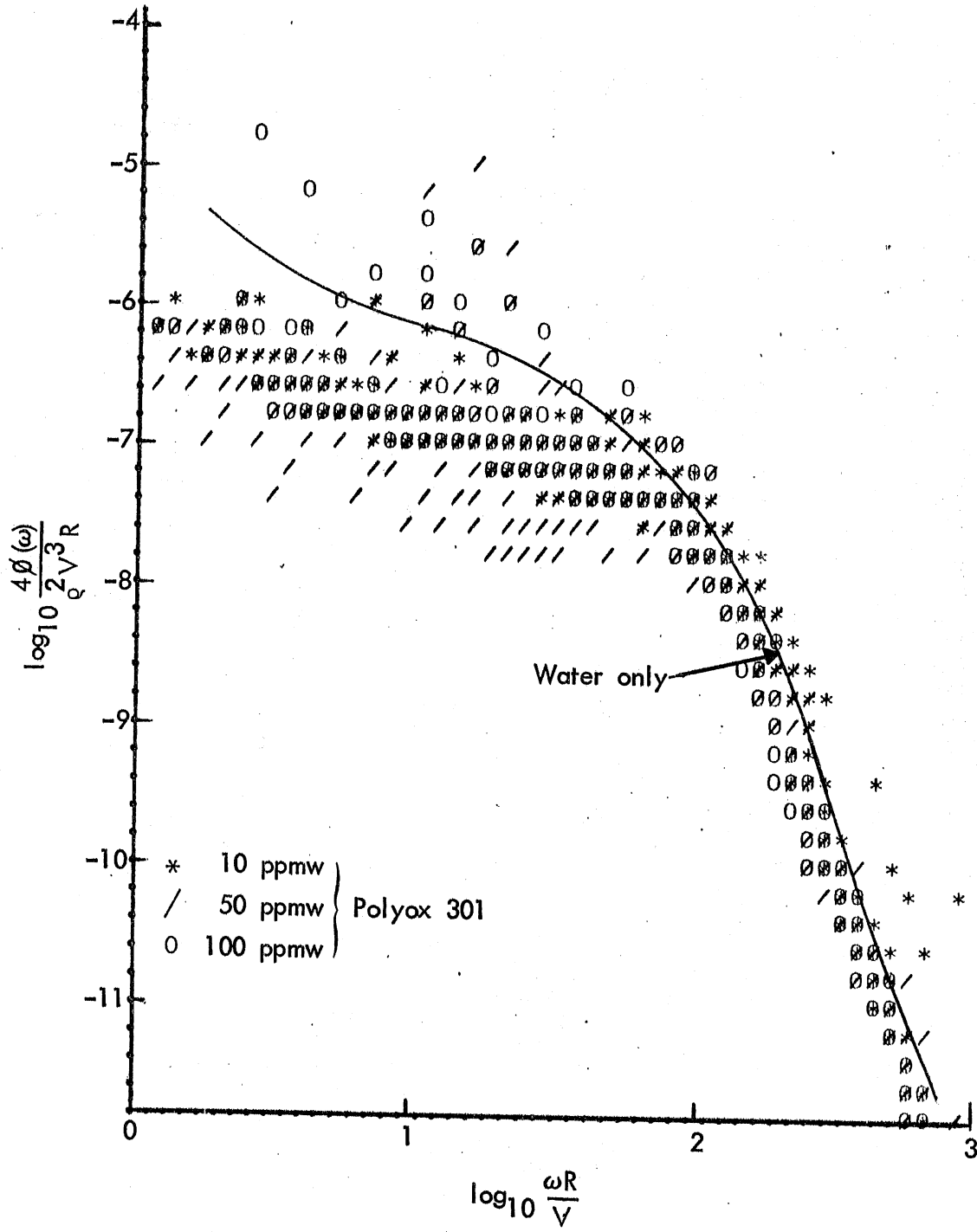


Fig. 13 - Surface Pressure Fluctuation Spectra on a Smooth Surface with various concentrations of Polyox 301

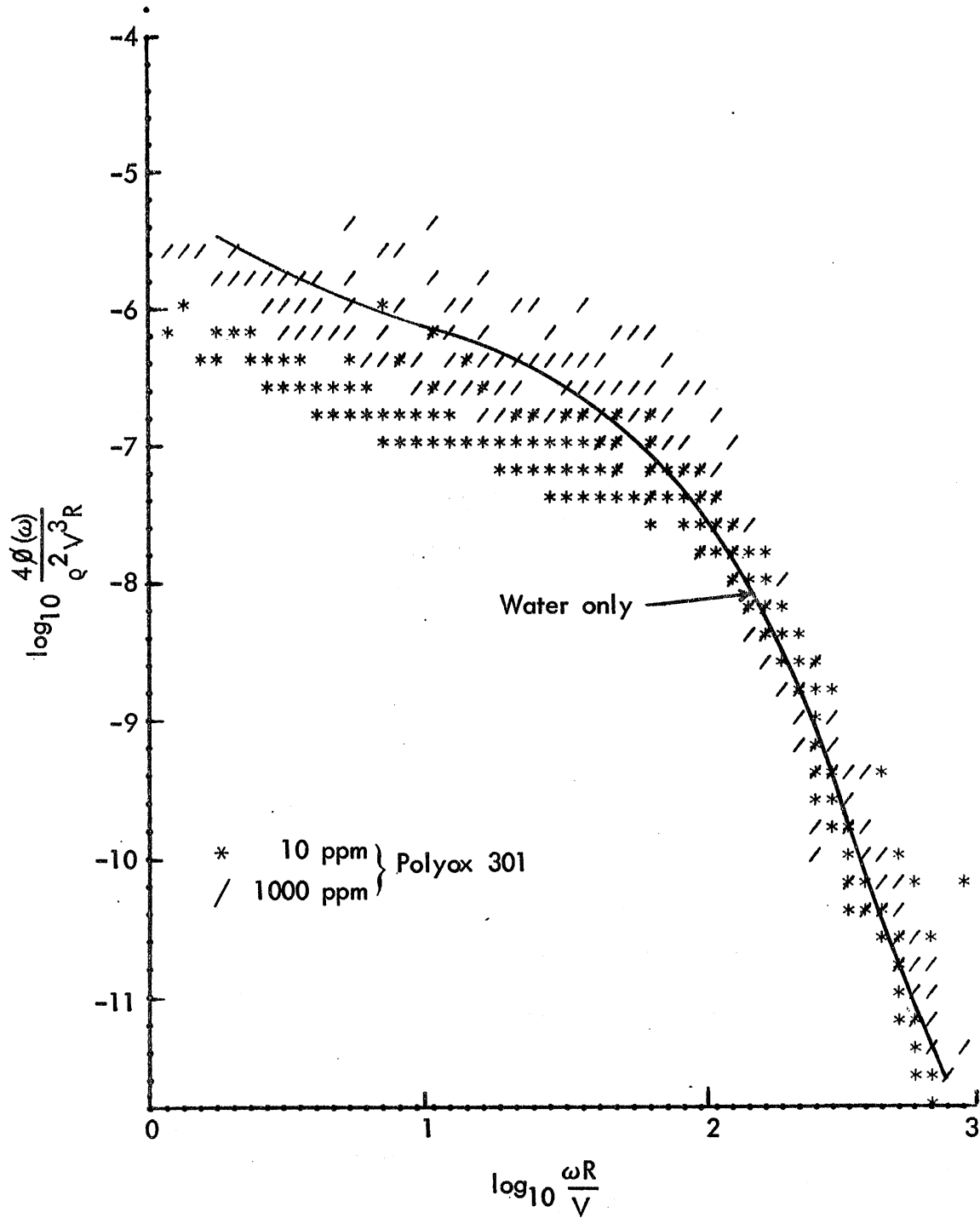


Fig. 14 - Surface Pressure Fluctuation Spectra on a Smooth Surface with Large Change in Polyox 301 Concentration

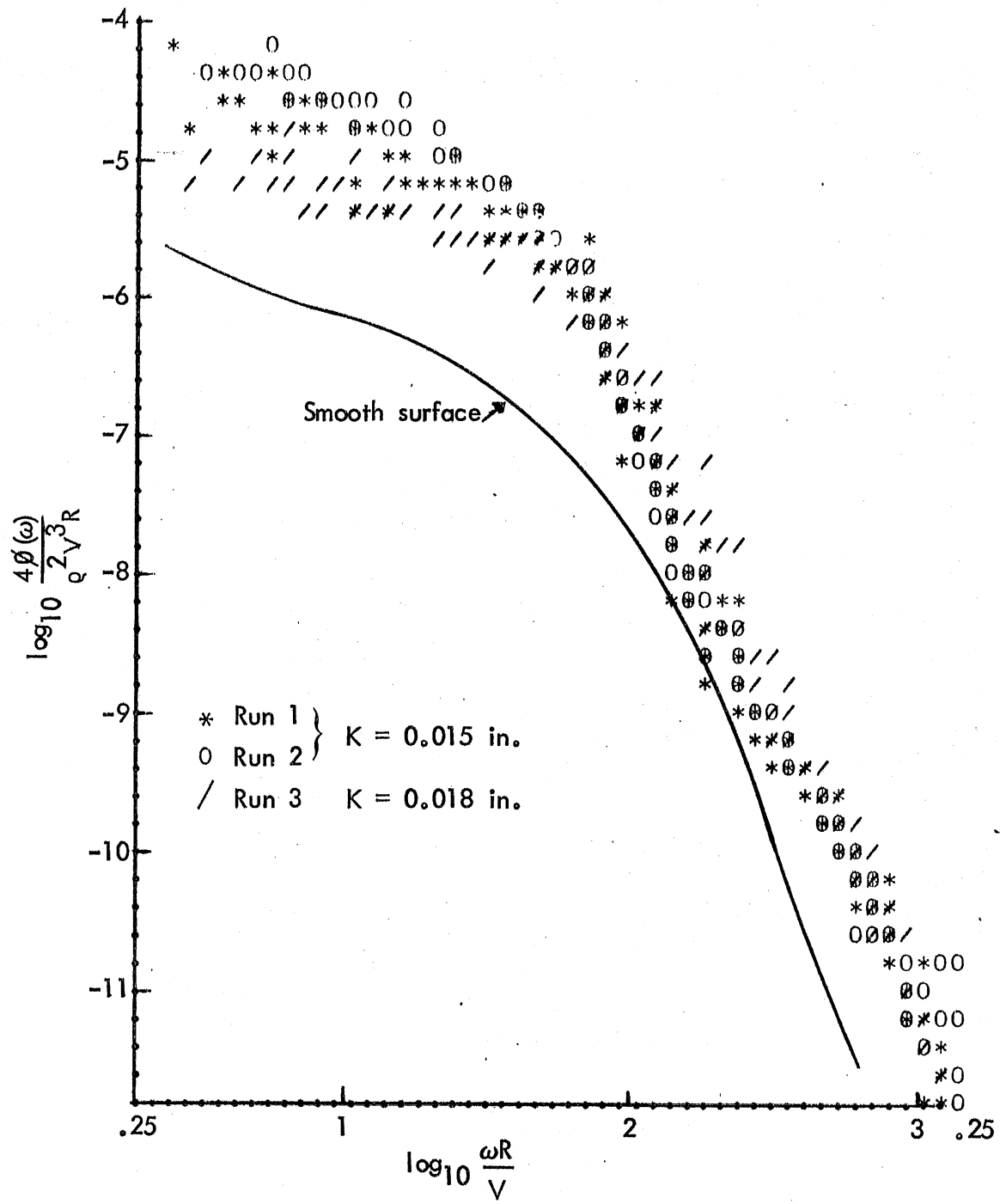


Fig. 15 - Surface Pressure Fluctuation Spectra on Rough Surfaces - Water

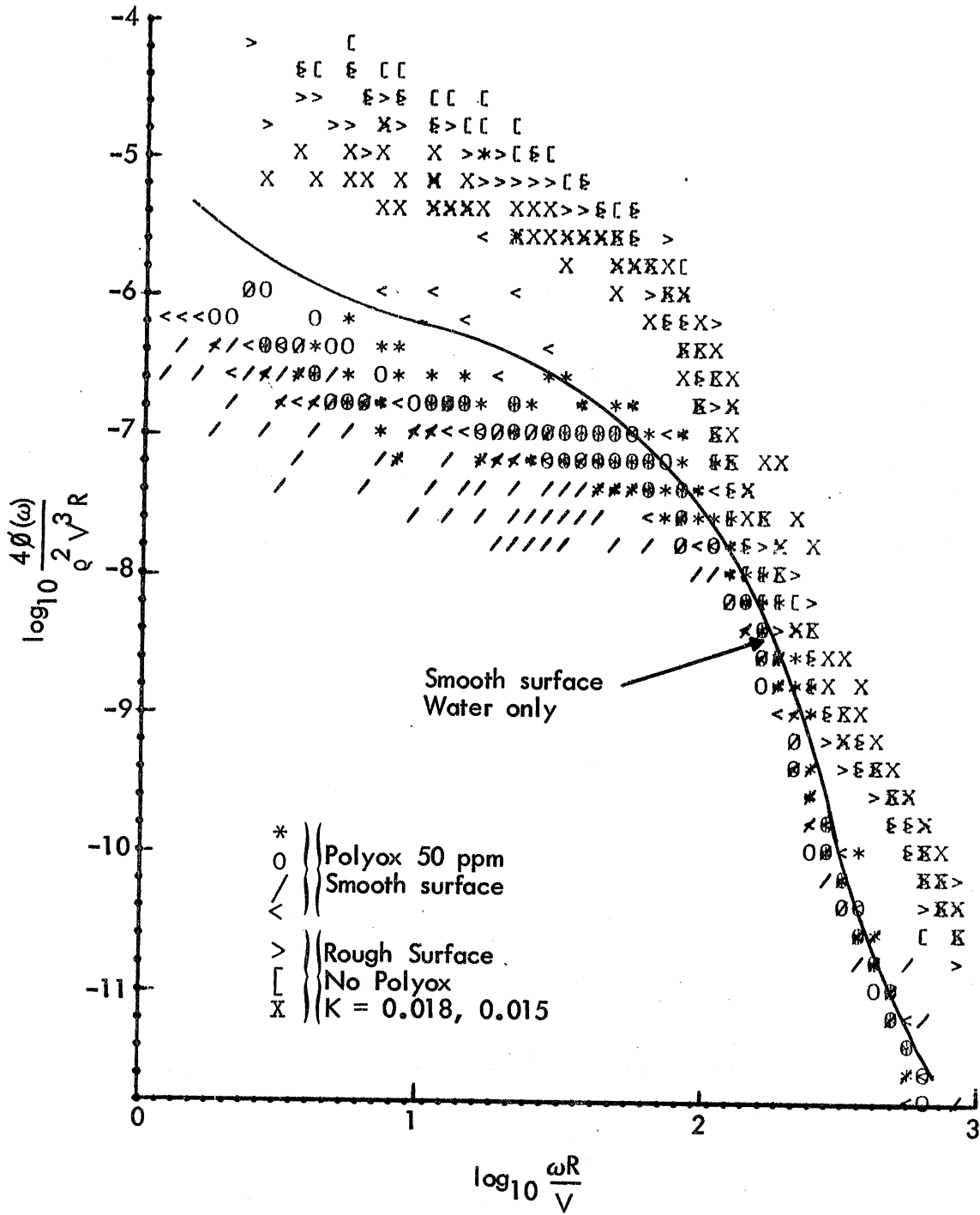


Fig. 16 - Surface Pressure Fluctuation Spectra - Comparison of Roughness and Additive with Smooth Surface Condition

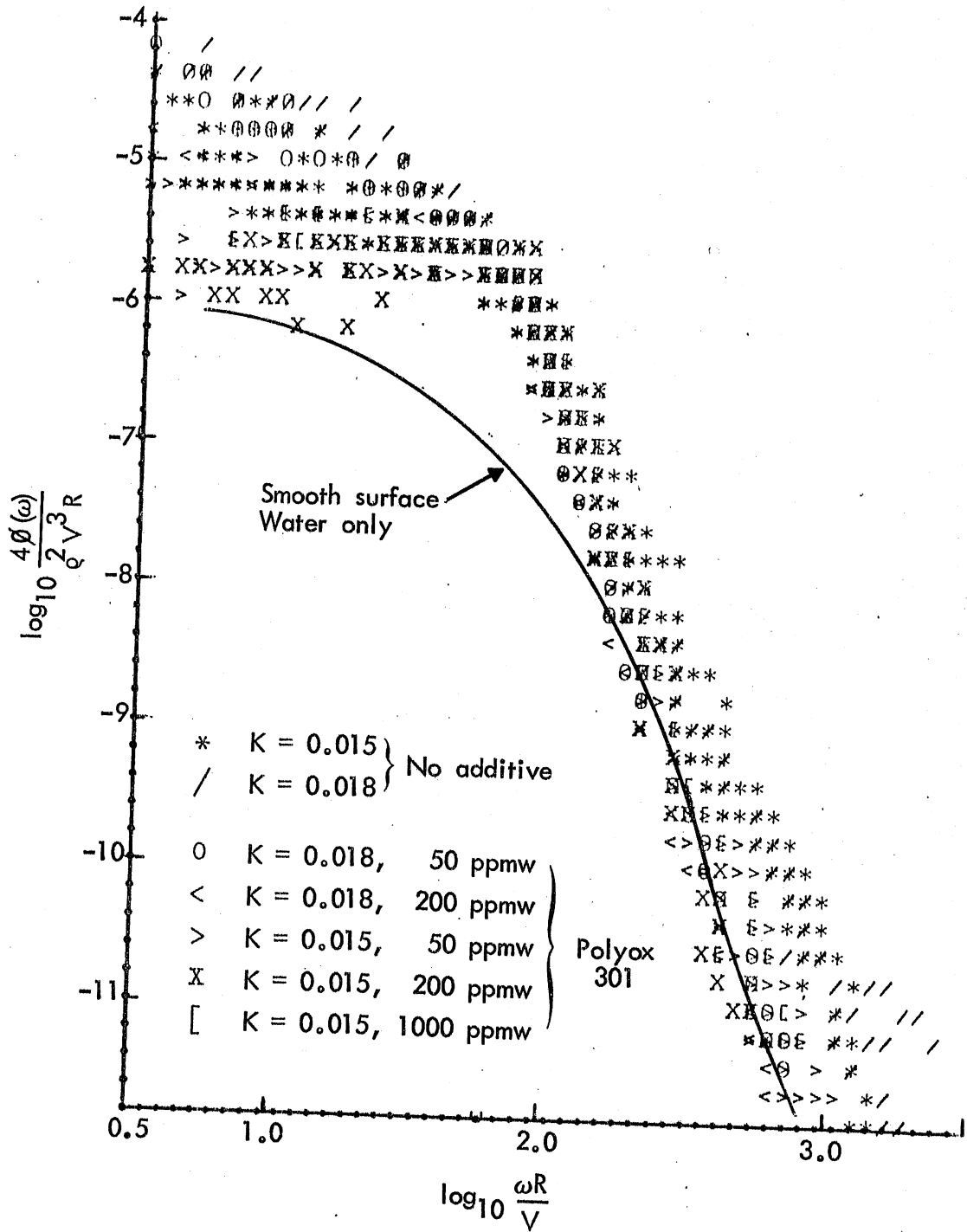


Fig. 17 - Surface Pressure Fluctuation Spectra on a Rough Surface with various concentrations of Polyox 301

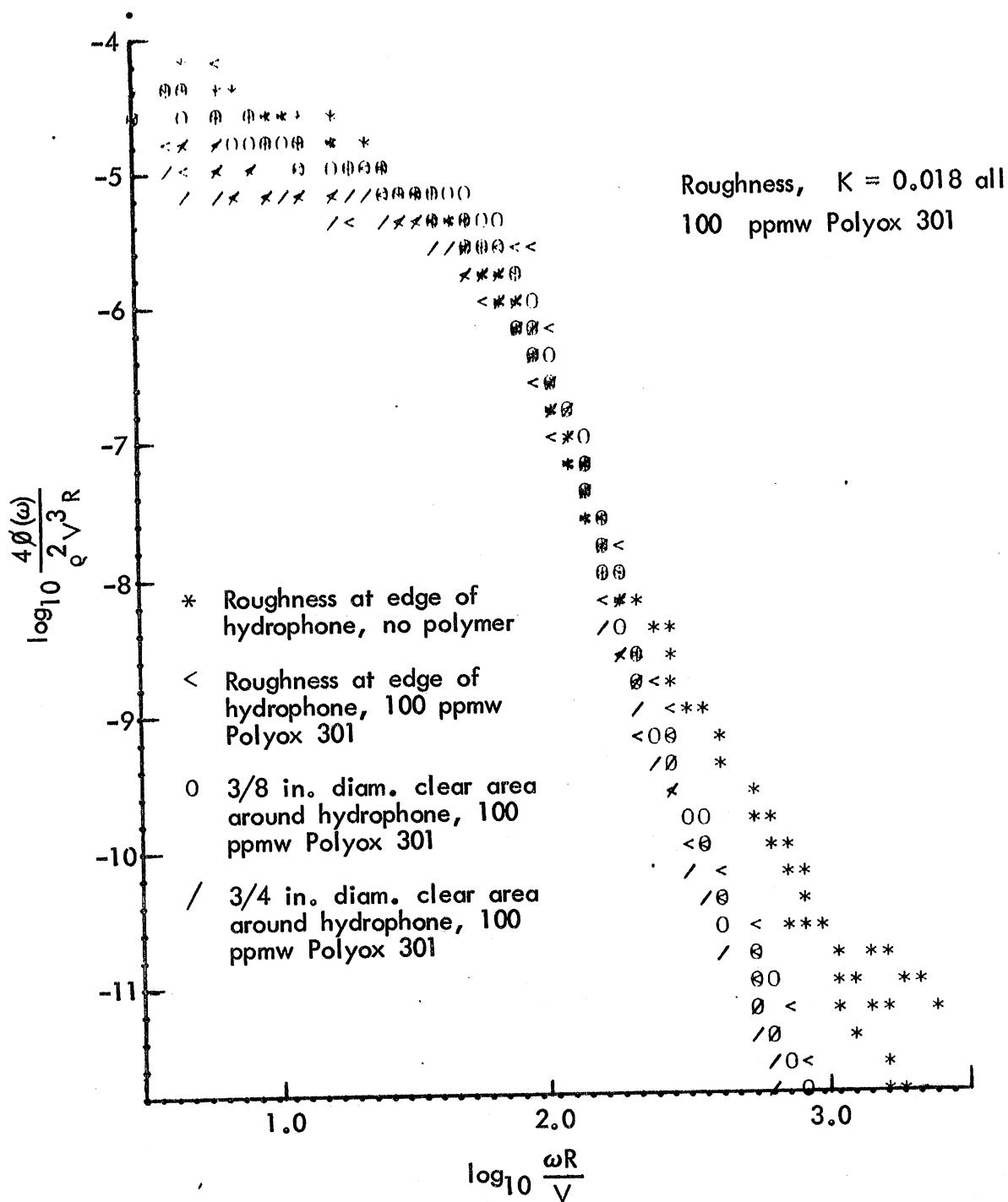


Fig. 18 - Surface Pressure Fluctuation Spectra - Interaction between Roughness and Hydrophone in the presence of Polymer - Roughness $K = 0.018$, 100 ppmw Polyox 301

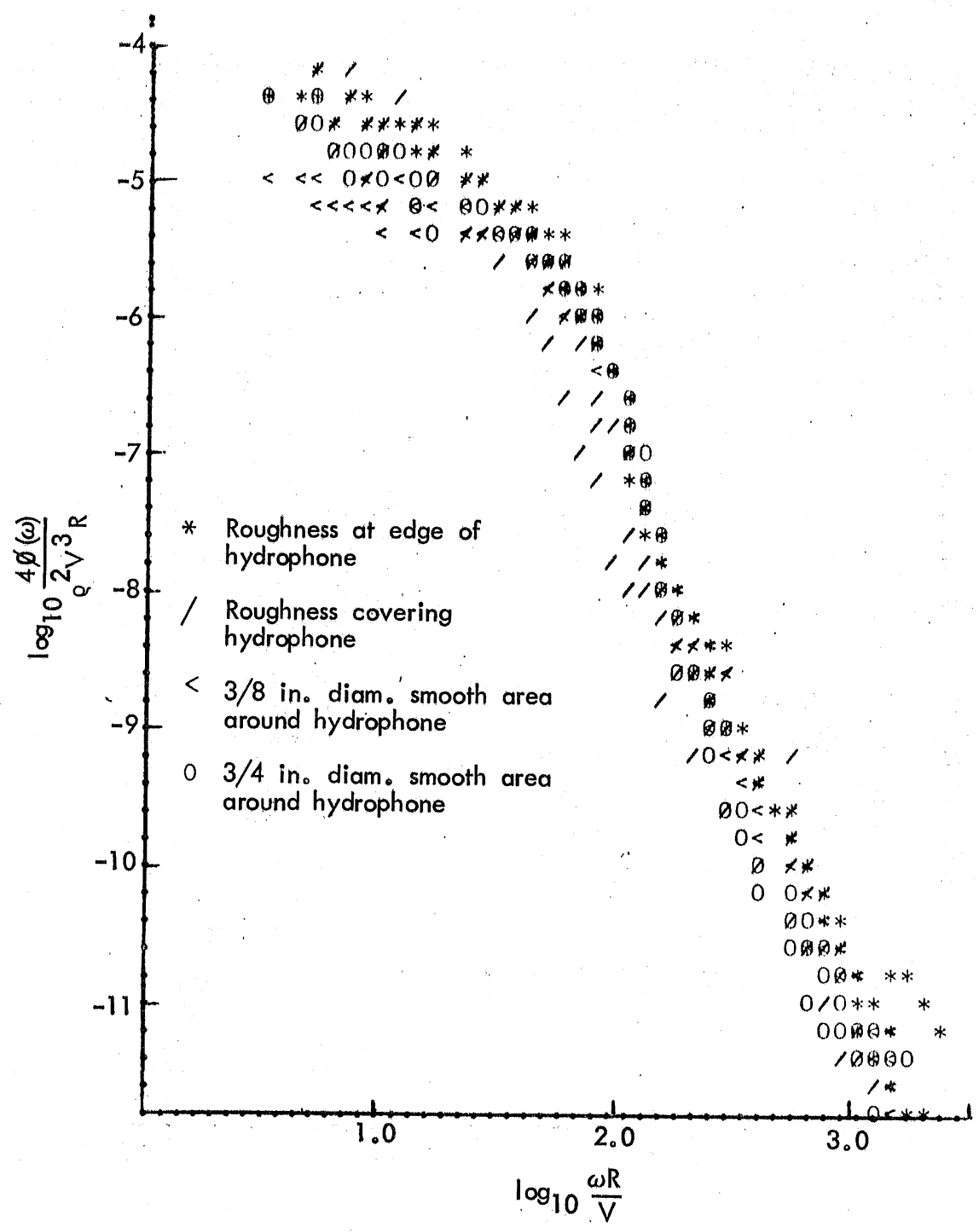


Fig. 19 - Surface Pressure Fluctuation Spectra Interaction between Roughness and Hydrophone in Water Only, Roughness K = 0.018

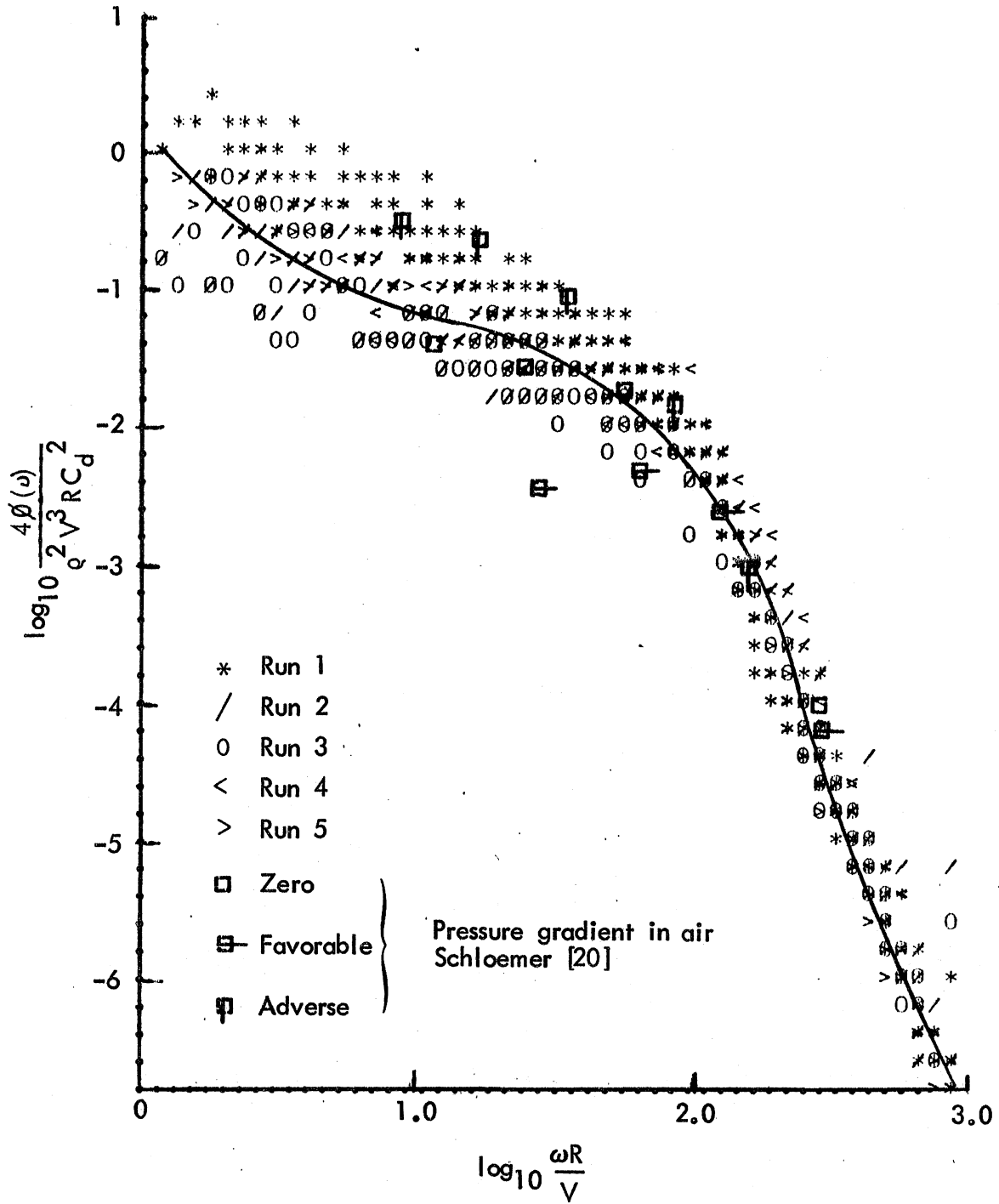


Fig. 20 - Surface Pressure Fluctuation Spectra on a Smooth Surface - Water Only

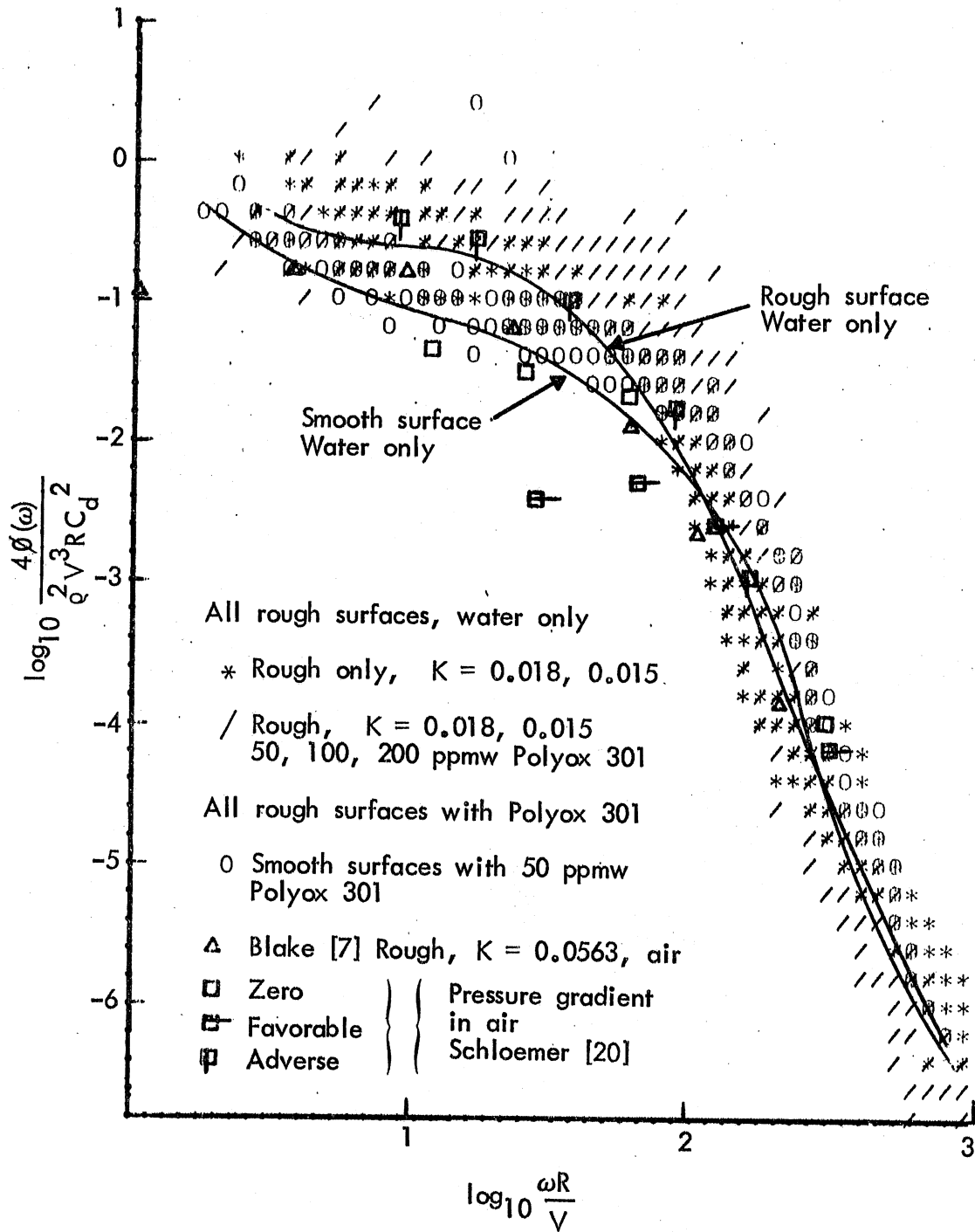


Fig. 21 - Surface Pressure Fluctuation Spectra as Influenced by Roughness and Drag Reducing Additive

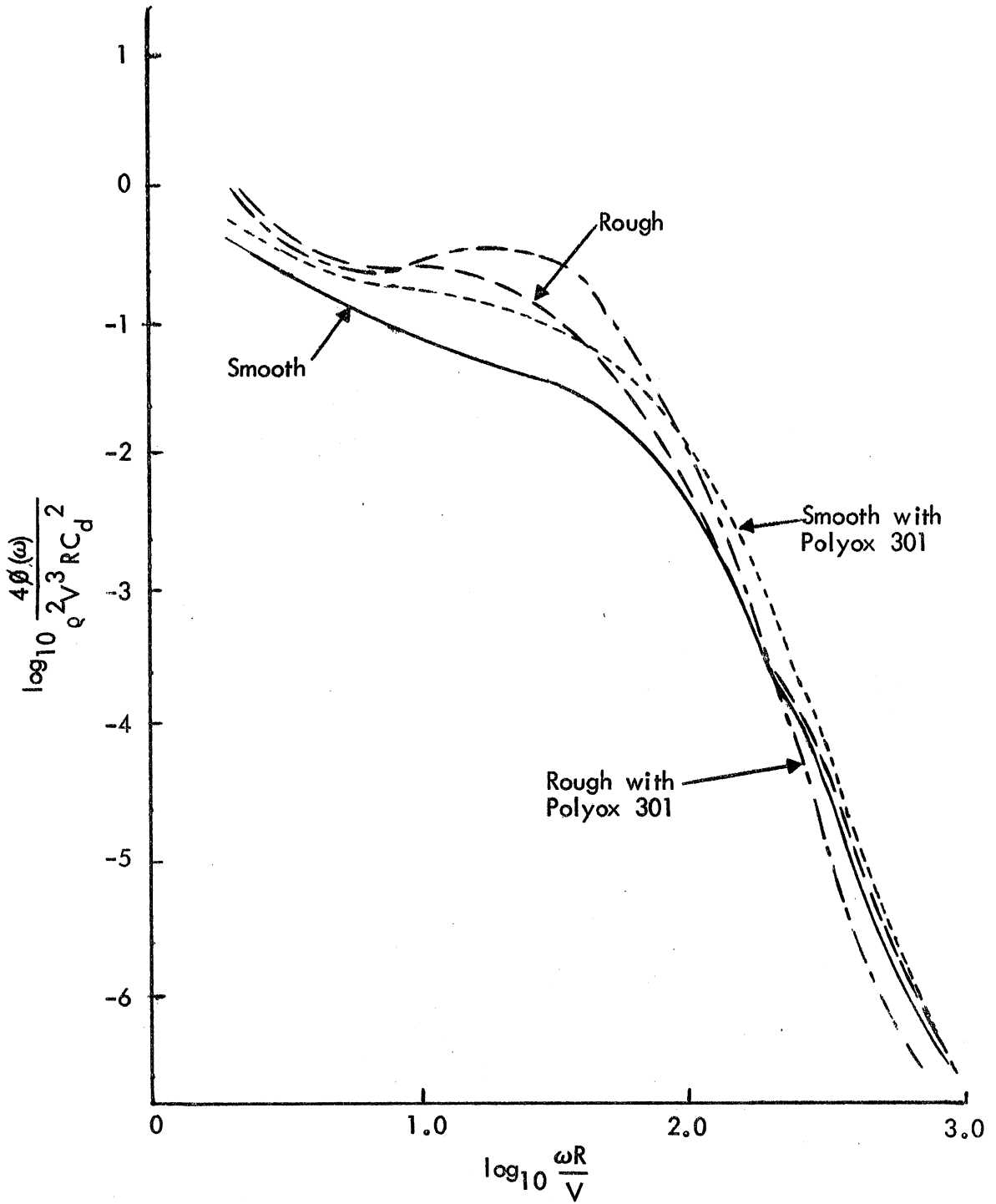


Fig. 22 - Comparison of "Fitted" Curves to Four Experimental Conditions

DISTRIBUTION LIST FOR PROJECT REPORT NO. 119
of the St. Anthony Falls Hydraulic Laboratory

Copies

Organization

- 40 Commander, Naval Ship Research and Development Center, Bethesda, Maryland 20034, Attn:
Code 1505
Code 5614 (39)
- 1 Officer-in-Charge, Annapolis Laboratory, Naval Ship Research and Development Center, Annapolis, Maryland 21402, Attn: Code 5642 (Library)
- 5 Commander, Naval Ship Systems Command, Washington, D. C. 20360, Attn:
SHIPS 2052 (3)
SHIPS 03412B
SHIPS 0372
- 12 Director, Defense Documentation Center, 5010 Duke Street, Alexandria, Virginia 22314
- 1 Office of Naval Research, 800 N. Quincy Street, Arlington, Virginia 22217, Attn: Mr. R. D. Cooper (Code 438)
- 1 Office of Naval Research Branch Office, 492 Summer Street, Boston, Mass. 02210
- 1 Office of Naval Research Branch Office (493), 536 S. Clark Street, Chicago, Illinois 60605
- 1 Chief Scientist, Office of Naval Research Branch Office, 1030 E. Green Street, Pasadena, California 91106
- 1 Office of Naval Research Resident Representative, 207 West 24th Street, New York, New York 10011
- 1 Office of Naval Research Resident Representative, 50 Fell Street, San Francisco, CA 94102
- 2 Director, Naval Research Laboratory, Washington, D. C. 20390, Attn:
Code 2027
Code 2629 (ONRL)
- 1 Commander, Naval Facilities Engineering Command (Code 032C), Washington, D.C. 20390
- 1 Library of Congress, Science and Technology Division, Washington, D.C. 20540
- 1 Commander, Naval Ordnance Systems Command (ORD 035), Washington, D.C. 20360
- 1 Commander, Naval Electronics Laboratory Center (Library), San Diego, CA 92152

Copies

- 8 Commander, Naval Ship Engineering Center, Center Building, Prince Georges Center, Hyattsville, Maryland 20782, Attn:
 SEC 6034B SEC 6136
 SEC 6110 SEC 6144G
 SEC 6114H SEC 6140B
 SEC 6120 SEC 6148
- 1 Library (Code 1640), Naval Oceanographic Office, Washington, D.C. 20390
- 1 Technical Library, Naval Proving Ground, Dahlgren, Virginia 22448
- 1 Commander (ADL), Naval Air Development Center, Warminster, Penna 18974
- 1 Naval Underwater Weapons Research and Engineering Station (Library), Newport, R. I. 02840
- 1 Commanding Officer (L31), Naval Civil Engineering Laboratory, Port Hueneme, CA 93043
- 1 Commander, Naval Undersea Research and Development Center, San Diego, CA 92132, Attn: Dr. A. Fabula (6005)
- 2 Officer-in-Charge, Naval Undersea Research and Development Center, Pasadena, CA 91107, Attn:
 Dr. J. Hoyt (2501)
 Library (13111)
- 1 Director, Naval Research Laboratory, Underwater Sound Reference Division, P.O. Box 8337, Orlando, Florida 32806
- 1 Library, Naval Underwater Systems Center, Newport, R. I. 02840
- 1 Research Center Library, Waterways Experiment Station, Corps of Engineers, P.O. Box 631, Vicksburg, Mississippi 39180
- 2 National Bureau of Standards, Washington, D.C. 20234, Attn:
 P. Klebanoff (FM 105), Fluid Mechanics
 Hydraulic Section
- 1 AFOSR/NAM, 1400 Wilson Blvd, Arlington, Virginia 22209
- 1 AFFOL/FYS (J. Olsen), Wright Patterson AFB, Dayton, Ohio 45433
- 1 Dept. of Transportation, Library TAD-491.1, 400 - 7th Street S.W., Washington, D. C. 20590
- 1 Boston Naval Shipyard, Planning Dept. Bldg. 39, Technical Library, Code 202.2, Boston, Mass. 02129
- 1 Charleston Naval Shipyard, Technical Library, Naval Base, Charleston, South Carolina 29408

Copies

- 1 Norfolk Naval Shipyard, Technical Library, Portsmouth, Virginia 23709
- 1 Philadelphia Naval Shipyard, Philadelphia, Penna. 19112, Attn:
Code 240
- 1 Portsmouth Naval Shipyard, Technical Library, Portsmouth, N. H.
03801
- 1 Puget Sound Naval Shipyard, Engineering Library, Bremerton, Wash.
98314
- 1 Long Beach Naval Shipyard, Technical Library (246L), Long Beach, CA
90801
- 1 Hunters Point Naval Shipyard, Technical Library (Code 202.3), San
Francisco, CA 94135
- 1 Pearl Harbor Naval Shipyard, Code 202.32, Box 400, FPO, San Francisco,
CA 96610
- 1 Mare Island Naval Shipyard, Shipyard Technical Library, Code 202.3,
Vallejo, CA 94592
- 1 Assistant Chief Design Engineer for Naval Architecture (Code 250),
Mare Island Naval Shipyard, Vallejo, CA 94592
- 3 U.S. Naval Academy, Annapolis, Maryland 21402, Attn:
Technical Library
Dr. Bruce Johnson
Prof. P. Van Mater, Jr.
- 3 Naval Postgraduate School, Monterey, CA 93940, Attn:
Library, Code 2124
Dr. T. Sarpkaya
Prof. J. Miller
- 1 Capt. L. S. McCready, USMS, Director, National Maritime Research
Center, U.S. Merchant Marine Academy, Kings Point, L.I., N.Y. 11204
- 1 U.S. Merchant Marine Academy, Kings Point, L.I., N.Y. 11204, Attn:
Academy Library
- 1 Library, The Pennsylvania State University, Ordnance Research
Laboratory, P.O. Box 30, State College, Penna. 16801
- 1 Bolt, Beranek and Newman, 1501 Wilson Blvd., Arlington, Virginia
22209, Attn: Dr. F. Jackson
- 1 Bolt, Beranek and Newman, 50 Moulton Street, Cambridge, Mass. 02138,
Attn: Library
- 1 Bethlehem Steel Corporation, Center Technical Division, Sparrows
Point Yard, Sparrows Point, Maryland 21219

Copies

- 1 Bethlehem Steel Corporation, 25 Broadway, New York, New York 10004,
Attn: Library (Shipbuilding)
- 1 Cambridge Acoustical Associates, Inc., 1033 Mass. Avenue, Cambridge,
Mass., 02138, Attn: Dr. M. Junger
- 1 Cornell Aeronautical Laboratory, Aerodynamics Research Dept., P.O.
Box 235, Buffalo, N.Y. 14221, Attn: Dr. A. Ritter
- 1 Eastern Research Group, P.O. Box 222, Church Street Station, New York,
New York 10008
- 1 Esso International, Design Division, Tanker Dept., 15 West 51st Street,
New York, New York 10019
- 1 Mr. V. Boatwright, Jr., R and D Manager, Electric Boat Division, General
Dynamics Corporation, Groton, Conn. 06340
- 1 Gibbs and Cox, Inc., Technical Information Control Section, 21 West
Street, New York, New York 10006
- 1 Hydronautics, Inc., Pindell School Road, Howard County, Laurel, Maryland
20810, Attn: Library
- 2 McDonnell Douglas Aircraft Co., 3855 Lakewood Blvd., Long Beach, CA
90801, Attn:
 J. Hess
 A. M. O. Smith
- 1 Lockheed Missiles and Space Co., P.O. Box 504, Sunnyvale, CA 94088,
Attn: Mr. R. L. Waid, Dept. 57-74, Bldg. 150, Facility 1
- 1 Newport News Shipbuilding and Dry Dock Company, 4101 Washington Avenue,
Newport News, Virginia 23607, Attn: Technical Library Dept.
- 1 North American Aviation, Inc., Space and Information Systems Div.,
12214 Lakewood Blvd., Downey, CA 90241, Attn: Mr. Ben Ujihara (SL-20)
- 1 Nielsen Engineering and Research, Inc., 850 Maude Avenue, Mountain View,
CA 94040, Attn: Mr. S. B. Spangler
- 1 Oceanics, Inc., Technical Industrial Park, Plainview, L.I., N.Y. 11803
- 1 Society of Naval Architects and Marine Engineers, 74 Trinity Place,
New York, New York 10006, Attn: Technical Library
- 1 Sperry Systems Management Division, Sperry Rand Corporation, Great
Neck, N. Y. 11020, Attn: Technical Library
- 1 Stanford Research Institute, Menlo Park, CA 94025, Attn: Library
G-021

Copies

- 2 Southwest Research Institute, P.O. Drawer 28510, San Antonio,
Texas 78284, Attn:
Applied Mechanics Review
Dr. H. Abramson
- 1 Tracor, Inc., 6500 Tracor Lane, Austin, Texas 78721
- 1 Mr. Robert Taggart, 3930 Walnut Street, Fairfax, Virginia 22030
- 1 Ocean Engr. Department, Woods Hole Oceanographic Institute,
Woods Hole, Massachusetts 02543
- 1 Worcester Polytechnic Institute, Alden Research Laboratories,
Worcester, Mass. 01609, Attn: Technical Library
- 1 Applied Physics Laboratory, University of Washington, 1013 N.E.
40th Street, Seattle, Washington 98105, Attn: Technical Library
- 1 University of Bridgeport, Bridgeport, Conn. 06602, Attn: Dr.
E. Uram
- 1 Cornell University, Graduate School of Aerospace Engr., Ithaca,
New York 14850, Attn: Prof. W. R. Sears
- 4 University of California, Naval Architecture Department, College of
Engineering, Berkeley, CA 94720, Attn:
Library
Prof. W. Webster
Prof. J. Paulling
Prof. J. Wehausen
- 3 California Institute of Technology, Pasadena, CA 91109, Attn:
Aeronautics Library
Dr. T. Y. Wu
Dr. A. J. Acosta
- 1 Docs/Repts/Trans Section, Scripps Institution of Oceanography
Library, University of California, San Diego, P.O. Box 2367,
La Jolla, CA 92037
- 1 Catholic University of America, Washington, D. C. 20017, Attn:
Dr. S. Heller, Dept. of Civil and Mech. Engr.
- 1 Colorado State University, Foothills Campus, Fort Collins, Colorado
80521, Attn: Reading Room, Engr. Res. Center
- 1 University of California at San Diego, La Jolla, CA 92038, Attn:
Dr. A. T. Ellis, Dept. of Applied Math.
- 1 Florida Atlantic University, Ocean Engineering Department, Boca
Raton, Fla 33432, Attn: Technical Library

Copies

- 2 Harvard University, Pierce Hall, Cambridge, Mass. 02138, Attn:
Prof. G. Carrier
Gordon McKay Library
- 1 University of Hawaii, Department of Ocean Engineering, 2565 The Mall,
Honolulu, Hawaii 96822, Attn: Dr. C. Bretschneider
- 1 University of Illinois, Urbana, Illinois 61801, Attn: Dr. J.
Robertson
- 3 Institute of Hydraulic Research, The University of Iowa, Iowa City,
Iowa 52240, Attn:
Library
Dr. L. Landweber
Dr. J. Kennedy
- 1 The Johns Hopkins University, Baltimore, Md. 21218, Attn: Prof. O.
Phillips, Mechanics Department
- 1 Kansas State University, Engineering Experiment Station, Seaton Hall,
Manhattan, Kansas 66502, Attn: Prof. D. Nesmith
- 1 University of Kansas, Chm. Civil Engineering Dept. Library, Lawrence,
Kansas 60644
- 5 Department of Ocean Engineering, Massachusetts Institute of Technology,
Cambridge, Mass. 02139, Attn:
Department Library
Prof. P. Leehey
Prof. P. Mandel
Prof. M. Abkowitz
Dr. J. Newman
- 1 Parsons Laboratory, Massachusetts Institute of Technology, Cambridge,
Mass. 02139, Attn: Prof. A. Ippen
- 5 St. Anthony Falls Hydraulic Laboratory, University of Minnesota, Missis-
sippi River at 3rd Avenue S.E., Minneapolis, Minnesota 55414, Attn:
Mr. J. Wetzel
Dr. F. Schiebe
Dr. J. Killen
Dr. C. C. S. Song
- 3 Department of Naval Architecture and Marine Engineering, University of
Michigan, Ann Arbor, Michigan 48104, Attn:
Library
Dr. T. F. Ogilvie
Prof. F. Hammitt
- 2 College of Engineering, University of Notre Dame, Notre Dame, Indiana 46556,
Attn:
Engineering Library
Dr. A. Strandhagen

Copies

- 2 New York University, Courant Inst. of Math. Sciences, 251 Mercier Street, New York, New York 10012, Attn:
Prof. A. Peters
Prof. J. Stoker
- 1 New York University, University Heights, Bronx, New York 10453,
Attn: Prof. W. Pierson, Jr.
- 1 Department of Aerospace and Mechanical Sciences, Princeton University,
Princeton, N.J. 08540, Attn: Prof. G. Mellor
- 3 Davidson Laboratory, Stevens Institute of Technology, 711 Hudson Street, Hoboken, New Jersey 07030, Attn:
Library
Mr. J. Breslin
Mr. S. Tsakonas
- 1 Department of Mathematics, St. John's University, Jamaica, New York 11432, Attn: Prof. J. Lurye
- 1 Applied Research Laboratory Library, University of Texas, P.O. Box 8029, Austin, Texas 78712
- 1 College of Engineering, Utah State University, Logan, Utah 84321,
Attn: Dr. R. Jeppson
- 2 Stanford University, Stanford, CA 94305, Attn:
Engineering Library
Dr. R. Street
- 3 Webb Institute of Naval Architecture, Crescent Beach Road, Glen Cover, L.I., N.Y. 11542, Attn:
Library
Prof. E. V. Lewis
Prof. L. W. Ward
- 1 National Science Foundation, Engineering Division Library, 1800 G Street N. W., Washington, D.C. 20550
- 1 University of Connecticut, Box U-37, Storrs, Conn. 06268, Attn:
Dr. V. Scottron, Hydraulic Research Lab
- 1 Long Island University, Graduate Department of Marine Science, 40 Merrick Avenue, East Meadow, L.I., N.Y. 11554, Attn: Prof. David Price

Unclassified

Security Classification

DOCUMENT CONTROL DATA - R & D

Security classification of title, body of abstract and indexing annotation must be entered when the overall report is classified

1. ORIGINATING ACTIVITY (Corporate author) St. Anthony Falls Hydraulic Laboratory University of Minnesota	2a. REPORT SECURITY CLASSIFICATION Unclassified 2b. GROUP
---	--

3. REPORT TITLE

THE INFLUENCE OF DRAG REDUCING POLYMER ADDITIVES ON SURFACE PRESSURE FLUCTUATIONS ON ROUGH SURFACES

4. DESCRIPTIVE NOTES (Type of report and, inclusive dates)
Project Report - November 1, 1967 through April 30, 1970

5. AUTHOR(S) (First name, middle initial, last name)
**John M. Killen
John A. Almo**

6. REPORT DATE September 1971	7a. TOTAL NO. OF PAGES 144	7b. NO. OF REFS 22
---	--------------------------------------	------------------------------

8a. CONTRACT OR GRANT NO. N00014-67-A-0113-0007 b. PROJECT NO. c. d.	9a. ORIGINATOR'S REPORT NUMBER(S) Project Report No. 119 9b. OTHER REPORT NO(S) (Any other numbers that may be assigned this report)
---	---

10. DISTRIBUTION STATEMENT

Approved for public release; distribution unlimited

11. SUPPLEMENTARY NOTES	12. SPONSORING MILITARY ACTIVITY Naval Ship Research and Development Center Bethesda, Maryland 20034
-------------------------	---

13. ABSTRACT

Experimental measurements were made to determine the effect of drag reducing polymer additives on the surface pressure fluctuations on smooth and rough surfaces in relative motion with water.

Changes in surface pressure fluctuation intensity, caused either by the addition of drag reducing polymer or by changes in surface roughness, or both, were found to correlate with changes in surface shear.

Unclassified

Security Classification

14

KEY WORDS

LINK A

LINK B

LINK C

ROLE

WT

ROLE

WT

ROLE

WT

Drag reducing polymer additives

Surface pressure fluctuations